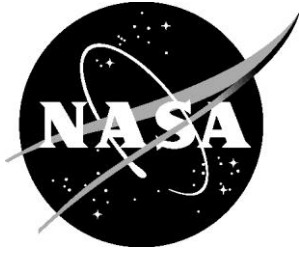


NASA/TM-2015-218784



Performance Comparisons and Down Selection of Small Motors for Two-Blade Heliogyro Solar Sail 6U CubeSat

*Peerawan Wiwattananon
National Institute of Aerospace, Inc., Hampton, Virginia*

*Robert G. Bryant
Langley Research Center, Hampton, Virginia*

August 2015

NASA STI Program . . . in Profile

Since its founding, NASA has been dedicated to the advancement of aeronautics and space science. The NASA scientific and technical information (STI) program plays a key part in helping NASA maintain this important role.

The NASA STI program operates under the auspices of the Agency Chief Information Officer. It collects, organizes, provides for archiving, and disseminates NASA's STI. The NASA STI program provides access to the NTRS Registered and its public interface, the NASA Technical Reports Server, thus providing one of the largest collections of aeronautical and space science STI in the world. Results are published in both non-NASA channels and by NASA in the NASA STI Report Series, which includes the following report types:

- **TECHNICAL PUBLICATION.** Reports of completed research or a major significant phase of research that present the results of NASA Programs and include extensive data or theoretical analysis. Includes compilations of significant scientific and technical data and information deemed to be of continuing reference value. NASA counter-part of peer-reviewed formal professional papers but has less stringent limitations on manuscript length and extent of graphic presentations.
- **TECHNICAL MEMORANDUM.** Scientific and technical findings that are preliminary or of specialized interest, e.g., quick release reports, working papers, and bibliographies that contain minimal annotation. Does not contain extensive analysis.
- **CONTRACTOR REPORT.** Scientific and technical findings by NASA-sponsored contractors and grantees.

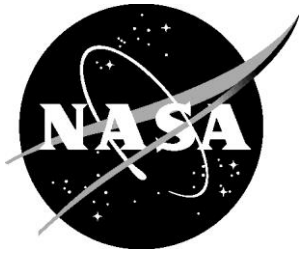
- **CONFERENCE PUBLICATION.** Collected papers from scientific and technical conferences, symposia, seminars, or other meetings sponsored or co-sponsored by NASA.
- **SPECIAL PUBLICATION.** Scientific, technical, or historical information from NASA programs, projects, and missions, often concerned with subjects having substantial public interest.
- **TECHNICAL TRANSLATION.** English-language translations of foreign scientific and technical material pertinent to NASA's mission.

Specialized services also include organizing and publishing research results, distributing specialized research announcements and feeds, providing information desk and personal search support, and enabling data exchange services.

For more information about the NASA STI program, see the following:

- Access the NASA STI program home page at <http://www.sti.nasa.gov>
- E-mail your question to help@sti.nasa.gov
- Phone the NASA STI Information Desk at 757-864-9658
- Write to:
NASA STI Information Desk
Mail Stop 148
NASA Langley Research Center
Hampton, VA 23681-2199

NASA/TM-2015-218784



Performance Comparisons and Down Selection of Small Motors for Two-Blade Heliogyro Solar Sail 6U CubeSat

*Peerawan Wiwattananon
National Institute of Aerospace, Inc., Hampton, Virginia*

*Robert G. Bryant
Langley Research Center, Hampton, Virginia*

National Aeronautics and
Space Administration

Langley Research Center
Hampton, Virginia 23681-2199

August 2015

The use of trademarks or names of manufacturers in this report is for accurate reporting and does not constitute an official endorsement, either expressed or implied, of such products or manufacturers by the National Aeronautics and Space Administration.

Available from:

NASA STI Program / Mail Stop 148
NASA Langley Research Center
Hampton, VA 23681-2199
Fax: 757-864-6500

Abstract

This report compiles a review of 130 commercial small scale (a volume within $3 \times 10^2 \text{ cm}^3$) piezoelectric and electric motors and almost 20 researched-grade small scale piezoelectric motors for potential use in a two-blade Heliogyro Solar Sail 6U CubeSat. In this application, a motor and gearhead will deploy a roll of solar sail thin film ($2 \mu\text{m}$ thick) accommodated in a 2U CubeSat ($100 \times 200 \times 100 \text{ mm}$). The application requirements are: space rated, output torque of 0.8 Nm, speed of 3 rpm, weight limited to 150 grams, diameter and length within 50 mm and 40 mm, respectively. The comparisons suggest that piezoelectric motors without a gearhead exhibit larger output torque with respect to their volume and weight and require less input power to produce high torque. A commercially available electric motor plus a gearhead was chosen through a proposed selection process to meet the application's design requirements. A piezoelectric motor without a gearhead was not chosen for this application due to no commercially available gearheads for piezoelectric motors.

1 Introduction

Motors convert electric energy into mechanical output. Electric motors use electromagnetic force to produce mechanical output, and can be classified based upon input electric current into DC and AC motors. Commercial electric motors include DC brushes, brushless and DC stepper motors. DC motors are of interest because of their overall simplified system architecture starting from a DC source that allow for applications in a confined space. Electric motors exhibit very high speed ranging from several thousand to more than 10^5 revolutions per minute, rpm [1–3]. Thus, electric motors with both low speed and high torque are usually unfavorable for most applications because they are larger, heavier, and more expensive [4]. In practice, a high speed motor is usually selected for low speed applications wherein a speed reduction mechanism, such as a gearbox (sometimes known as a gearhead) is used. However, more space and weight allowance is required for these transmission systems. In order to overcome this high speed mechanical reduction problem, and allow for high torque at low speed, a direct-drive motor is a good choice.

The most common direct drive motor used are piezoelectric motors, and piezoelectric ultrasonic motors because of low speed and high torque [5]. These devices are commonly referred to as ultrasonic motors as the resonance frequencies are typically in the ultrasonic range [6]. The principle of ultrasonic motors is to convert vibrational strain energy from the stator to mechanical rotational output at a rotor. The working principle of ultrasonic motors is governed by three major parts,

a high frequency power supply, a stator and a rotor. A stator, which is driven by a high frequency power supply, drives a rotor to produce mechanical output. In these motors, the permanent and electromagnets, found in the electric motors are replaced by piezoelectric ceramic elements. Here, the piezoelectric materials produce high force at low strains 0.01% across a broad frequency bandwidth. Thus, these piezoelectric based systems must operate at or near their resonance frequency in order to amplify their strain while limiting their power consumption. Watson et al. [7] showed that the force produced from a scaled down piezoelectric ultrasonic motors is larger than that produced by electric motors. Thus, mechanical speed reducers, such as gearheads, may not be necessary thereby simplifying their construction. For this reason, the use of piezoelectric ultrasonic motors, where direct drive is possible, is becoming more popular in applications ranging from medical, aeronautics, automotive, to precision positioning, etc.

This work describes the process used to select a drive system to deploy and control solar sail blades of a 6U CubeSat. Due to this specific application, the blade reel is a cylindrical shape limited to a diameter of approximately 80 mm, and the motors weight must be less than 150 grams. The paper then follows with a set of motor plus a gearhead selection methods to meet the requirements. Sets of motors and gearheads were analyzed and discussed, and the best drive system available was selected. The space-rated and non-space-rated commercial small scale DC motors presented in this paper are from Maxon Precision Motors [1], Precision Micro Drives [8], Johnson Electric [9], Crouzet [3] and AUTOM [2]. Commercial piezoelectric ultrasonic motors from FUKOKU-Shinsei [10] and PiezoMotor [11] and Johnson Electric [9] are also reviewed in this report. For ease of explanation, the term 'piezoelectric motor' will be used to represent both piezoelectric ultrasonic and piezoelectric motors.

2 Electric Motors and Piezoelectric Motors

The general aspects and characteristics of electric motors are presented in this section. Three electric motor types discussed are brushed, brushless, and stepper motors. The presentation is followed by a discussion of performance of commercial and state-of-the-art researched type piezoelectric motors.

Electric Motors

Conventional brushed DC motors are composed of an armature (rotor), commutator, brushes, and field windings that convert electrical energy into mechanical power through the use of both electro and permanent magnets. Brushed DC motors provide the smoothest drive amongst

the three electric motor types. However, cooling of these motors is not efficient because heat generated inside the motor cannot effectively dissipate to the surrounding environment due to windings and other parts inside the motor frame. This excessive heat accumulates and degrades the motor's performance by increasing the resistance of copper wires in the motor. Thus, more current is required to operate the motor to compensate for the increase in wire resistance, causing an additional increase in temperature of the motor. Lastly, continuous motor operation promotes wear at the brushes, and the resulting dust contaminates the internal working environment, further degrading performance.

Brushless (or *electric commutation*) DC motors do not contain brushes or a commutator; there is no direct contact to the rotor. Thus, less wear and friction affords a longer life time. Here, the windings are placed in the stator. Without brushes inside the motor, the rotational speed limit increases. Thus, brushless motors are suitable for very high speed applications. However, the cost of these brushless motors is comparatively expensive because of the use of rare earth magnets and complex electric circuitry.

Stepper motors provide a unique feature in that the output shaft rotates in a series of discrete angular intervals or steps; each step is taken as a command when an electric pulse is received. These motors are brushless, and are good for high-torque low-speed applications. There is little risk of overdriving a stepper motor due to large loads, or speeds; current is still needed to produce a holding torque [12]. Thus, heat will be generated and accumulate inside the motor at holding positions. This will lower the motor's efficiency and eventually shorten its life.

Piezoelectric Motors and Piezoelectric Ultrasonic Motors

Six piezoelectric motor concepts are discussed in this report: Piezo LEGS [11], wobble motion, travelling-wave, windmill, hybrid and a Langevin-type.

The general working principle of a piezoelectric ultrasonic motor is different than the electric motors discussed earlier, in that the motion generated from a piezoelectric ultrasonic motor is transferred through contact points between a stator and a rotor. Therefore, the motion relies upon friction and mechanical strain. A Piezo LEGS [11] walking principle relies on friction between the moving piezo legs and a rotor. When these piezo legs are electrically activated, they elongate and bend, Figure 1. Each piezo leg pair works together, alternately. When the first pair elongates and contacts the rotor, it pushes and displaces the rotor, while the second pair shrinks downward, Figure 1(a). The second pair then elongates and pushes the rotor further in another step, as the

first pair shrinks downward, Figure 1(b). When these pairs are activated out-of-phase at very high frequencies, many discrete movements of the rotor are generated appearing as smooth continuous motion.

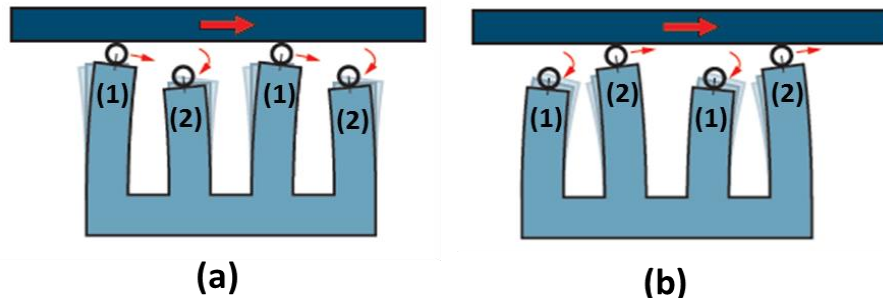


Figure 1. Piezo LEGS walking principle. Two leg pairs are shown in (a) and (b). (a) The first leg pair elongates upward and push the rotor to the right, while the second pair shrinks downward. (b) The second pair extends upward and displaces the rotor while the first pair shrink downward [11] *with permission from PiezoMotor*.

Another output motion of piezoelectric motor that is used by motor developers is a wobbling motion. The wobbling motion of a stator is generated by the rotational and bending motion, through actuation of a stator [13–15].

Examples of a wobbling motion of a stator include Moritas work on cylindrical tubes [16–20]. Another wobble motion motor developed by Koc et al. [21] attached two rectangular PZT plates on the side of an elastic hollow tube to produce a wobble motion. This produced a maximum output power of 60 mW and an efficiency of 25%. Later on, Cagatay et al. [22] minimized the motor dimension and produced an output power of 3.2 mW and an efficiency of 11%. Park and He [23] used a similar concept as Koc et al. [21] but by attaching four PZT rectangular plates on four sides of a brass tube,. The motor could generate two bending rotational modes using one driving signal producing wobble motion. The wobble motion from the brass stator tube forced the rotor to rotate and this rotation in turn forced the output shaft to rotate.

Table 1 summaries rotary motors with a wobbling concept. Some of the observations from a wobbling concept with the same materials (PZT and a titanium tube) [16,18] show that by doubling the motor dimension, the output speed does not double, but increases by only 17% (from 680 rpm to 800 rpm); while the output torque does not show a significant change at all (from 0.67 μNm to 0.7 μNm). When comparing the motor with a stator made purely of bulk PZT [17] to one with a stator made of a mixture of bulk PZT and titanium [17], the motor with a pure bulk PZT shows a significant increase in output torque (from 0.7 μNm to 0.22 mNm).

Output Motion	Design Concept	Stator Materials	Maximum Speed [rpm]	Output Torque [Nm]	Dimension mm	References
Rotary	Wobbling	PZT		62×10^{-3}	$\phi 1.6 \times 4$	Cagatay et al. [22]
Rotary	Wobbling	PZT/metal	572	1.8×10^{-3}	$\phi 2.4 \times 10$	Koc et al. [21]
Rotary	Wobbling	PZT	650	0.22×10^{-3}	$\phi 2.4 \times 10$	Morita et al. [16]
Rotary	Wobbling	PZT/brass	1000	370×10^{-6}	$3.975 \times 3.975 \times 16$	Park and He [23]
Rotary	Wobbling	PZT/titanium	800	0.7×10^{-6}	$\phi 2.4 \times 10$	Morita et al. [16]
Rotary	Wobbling	PZT/titanium	680	0.67×10^{-6}	$\phi 1.4 \times 5$	Morita et al. [18]
Rotary	Wobbling	PZT	3850	0.025×10^{-6}	$\phi 2 \times 5.9$	Kanda et al. [19, 20]

Table 1. Summary of wobbling type motor design concept, materials, speed, output torque and dimensions.

A traveling-wave concept can be generated by superimposing two standing waves at the stator with a 90° phase difference. The traveling wave produces tangential movement at the stator and this movement causes tangential friction at the rotor, resulting in movement of the rotor, Figure 2. A ring-shaped stator traveling-wave type piezoelectric ultrasonic motor is used by FUKOKU-Shinsei [10] and Shinsei [24], Figure 3(a and b). A ring-shaped piezoelectric material is bonded to an elastic material to form a stator. The elastic material is fabricated with a number of teeth, known as projections, around the circumference. Their function is to improve the frictional coupling condition between the stator and a rotor. Thus, vibrations can be amplified at the vibration nodes on the stator to the rotor [25–30]. Zhang et al. [31] developed a travelling-wave type micro-motor using a miniature PZT-metal composite tube stator.

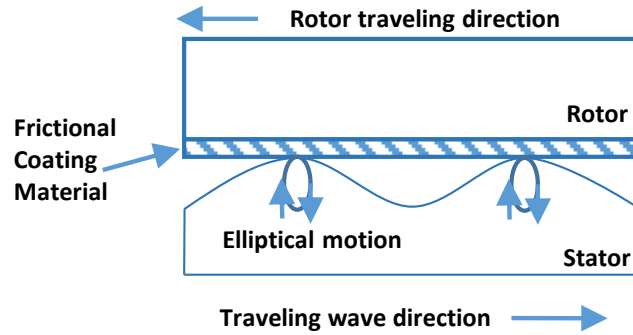


Figure 2. Traveling-wave motion principle.

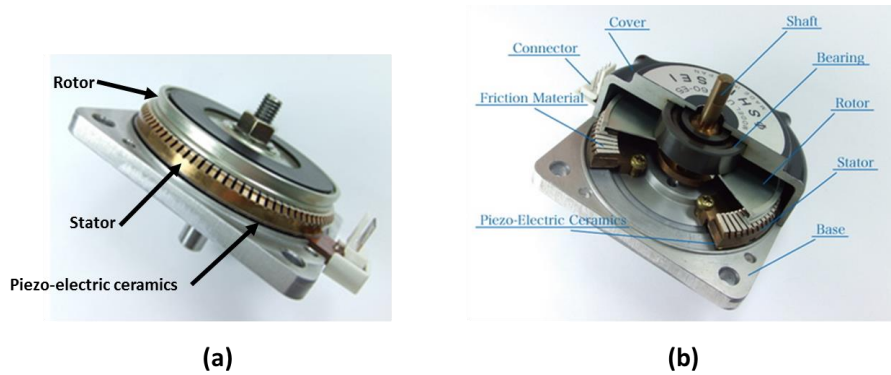


Figure 3. (a) Inside of a Shinsei piezoelectric ultrasonic motor, (b) a cut-through of a Shinsei piezoelectric ultrasonic motor [24].

A miniaturized "Windmill" concept ultrasonic micromotor was fabricated using a 60 vol% piezoelectric material and 40 vol% thermoplastic binder. This thermoplastic body was Computer Numerical Control (CNC-machined) to create windmill-type blades. The windmill stator

disk was poled in the thickness direction. With the application of an AC field in the thickness direction, the inward blades radial displacement generates tangential displacement to the rotor, causing the rotor to rotate [32].

Takeda et al. [33] developed a Langevin type motor with a piezoelectric ring. The motor had a diameter of 22 mm and 30.5 mm long. It could reach up to 293 rpm with an output torque of $5.7 \mu\text{Nm}$. Kurosawa and Ueha [34] developed a hybrid transducer type ultrasonic motor with longitudinal and torsional output motion. The stator was comprised of a bolted Langevin-type torsional transducer and three multilayered piezoelectric stack actuators between the rotor. The piezoelectric actuators produced longitudinal output motion along the motor axis to control frictional force at the rotor. A spring was used to provide a pre-load on the rotor. The torsional vibrator generated vibration through torsional piezoelectric plates. The two components, torsional vibrator and piezoelectric stack actuators, were independently driven by separate input electric sources. Similarly, Nakamura et al. [35] developed a hybrid transducer with longitudinal and torsional output motion. Wajchman et al. [36] developed a hybrid ultrasonic motor using a rectangular cross-sectioned pre-twisted beam stator made from aluminum.

It can be observed from Table 2 that the hybrid motor concept with a duralumin stator produced larger torque than the non-hybrid ones. This is because of a combination of motor motions, such as torsional and longitudinal that produces an output motion. These combinations improve the motor's output motion compared to those having only one motion.

Output Motion	Design Concept	Stator Materials	Maximum Speed [rpm]	Output Torque [Nm]	Dimension mm	References
Rotary	hybrid	PZT/duralumin	100	0.68	ϕ 50x82	Kurosawa and Ueha [34]
Rotary	hybrid	PZT/duralumin		0.29	ϕ 20x83	Nakamura et al. [35]
Rotary	windmill	PZT	156	22×10^{-6}	ϕ 5.2x0.6	Yoon et al. [32]
Rotary	travelling wave	PZT	3000	7.8×10^{-6}	ϕ 1x50	Zhang et al. [31]
Rotary	hybrid	PZT/Al	840	0.17×10^{-6}	6.5x6.5x87.5	Wajchman et al. [36]

Table 2. Summary of a travelling wave, windmill and hybrid motors and materials, speed, torque and dimension.

3 Performance Comparisons

This section compares and discusses the performance of motors presented in the preceding sections. The motor's performance are compared with volume within $3 \times 10^2 \text{ cm}^3$ and are extracted from scientific and product literature. The comparisons suggest that piezoelectric motors without a gearhead exhibit larger output torque with respect to their volume and weight and require less input power to produce high torque. Figure 4 to Figure 11 present commercial and research grade piezoelectric motors and commercial electric motors available on the market. Motor performance data are extracted from motor datasheet and cited literature. Thus, there is no gearhead affect in these data values. The output torque is of interest for the application that will be discussed later, wherein output torque will be discussed in terms of motor geometric characteristics in this report.

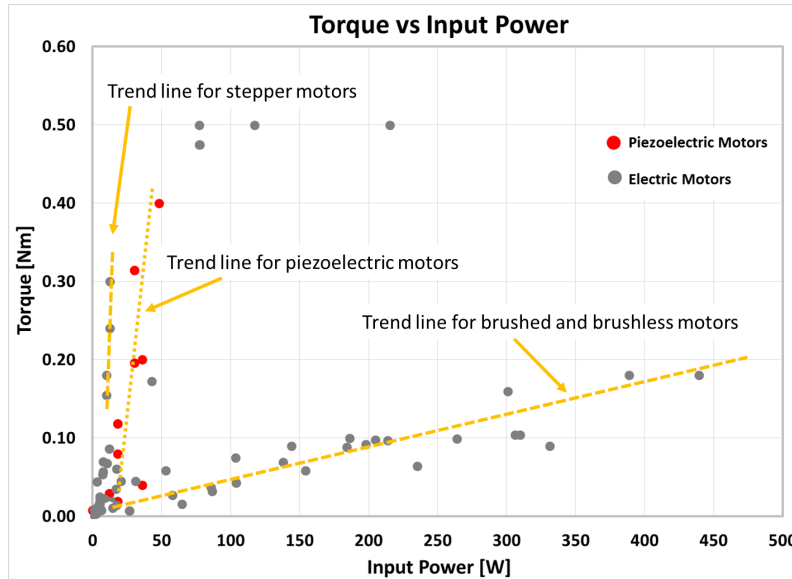


Figure 4. Output torque versus input power. Red dots represent piezoelectric motors. Grey dots represent electric motors. Three trend lines: 1) stepper motors trend line, 2) piezoelectric motors trend line and 3) brushed and brushless motors trend line, show how much torque the motors can produce with respect to input power. The two distinct trends (a trend line of brushes and brushless motors and the trend lines of stepper and piezoelectric motors) do not exhibit any physical meaning to the motor performance analysis. These two trends only represent available motor data for output torque versus input power.

Torque

The steeper trend line of piezoelectric motors versus trend line of brushed and brushless motors suggests that piezoelectric motors require less input power to produce output torque than brushed and brushless

motors, Figure 4. Stepper motors show a better trend (steeper slope) of output torque with respect to input power than other electric motors and piezoelectric motors, Figure 4. However, when considering the trend of torque density versus motor volume, piezoelectric motors suggest that they produce higher output torque density than most of the electric motors, Figure 5 and Figure 6.

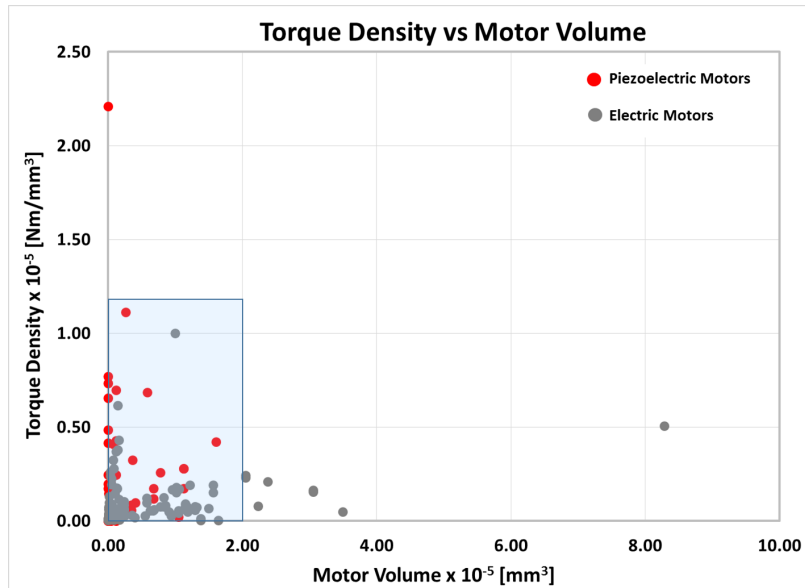


Figure 5. Torque density versus volume of the motor. Red dots represent piezoelectric motors. Grey dots represent electric motors. The shaded rectangular area includes motors that are going to be discussed further in Figure 6

At the larger motor volumes, piezoelectric ultrasonic motors show a higher trend of increased torque density. In general, the output torque from electric motors is in a direct relationship to the rotor volume and hence the motor volume [4]. However, these small scale electric motors do not seem to show the same relationship with motor volume. The two distinct data trends (a trend line of brushed and brushless motors and the trend lines of stepper and piezoelectric motors) in Figure 4 have no physical meaning against each other except that these are available motor data extracted from literature and commercial motor datasheets. Watson et al. [7] discussed effects of output force (hence it can be considered as output torque for a rotary motion) of electric motors when they are scaled down. They showed that the output force of miniature electric motors does not exhibit a direct relationship to the motor’s characteristic length, but it relates to the motor’s characteristic length to the power of four [37]. The output force of miniature piezoelectric motors shows a direct relationship to the motor’s characteristic length (Watson et al. [7]). The characteristic length is an input parameter in a scaling law that influences small scale system output behavior, for example, a

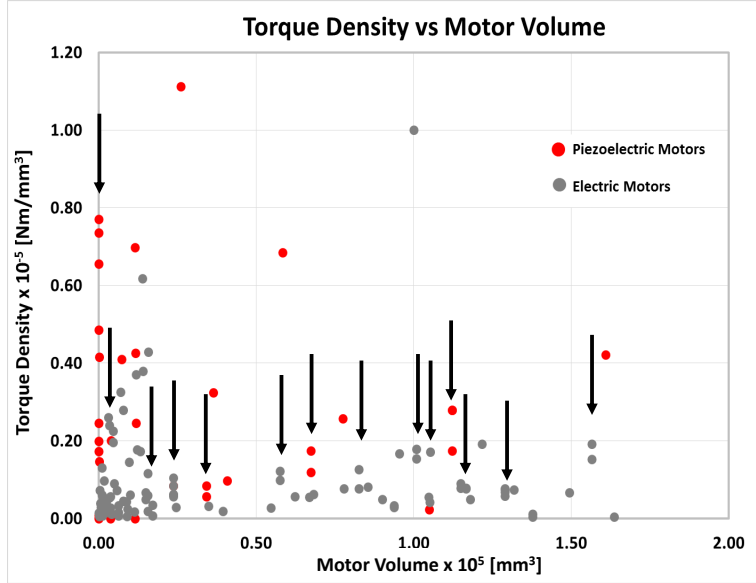


Figure 6. Torque density versus volume of the motor enlarged area from the shaded rectangular in Figure 5. Red dots represent piezoelectric motors. Grey dots represent electric motors. The arrows indicate groups of common motor volumes.

piezoelectric motor geometric parameter such as dimension of a piece of piezoelectric material inside the piezoelectric motor. From this scaling effect, piezoelectric motors are more competitive than electric motors in small scale applications since the smaller the motor, the lower the output force electric motors can produce due to the fourth power of the motor's characteristic length.

Besides the torque-volume density, when considering the motor's weight, piezoelectric motors exhibit a larger trend of torque-weight density than electric motors, Figures 7 and 8. The motors' weights presented here are too heavy (more than 3 kg) for applications that are going to be discussed later in the following section, thus, only motors' weights up to 500 grams are going to be considered here, Figure 8. When a motor's weight increases, the torque density of electric motor do not show significant increase; while piezoelectric motors exhibit a significant increase in the magnitude of torque-weight density at a higher weight range, Figure 8.

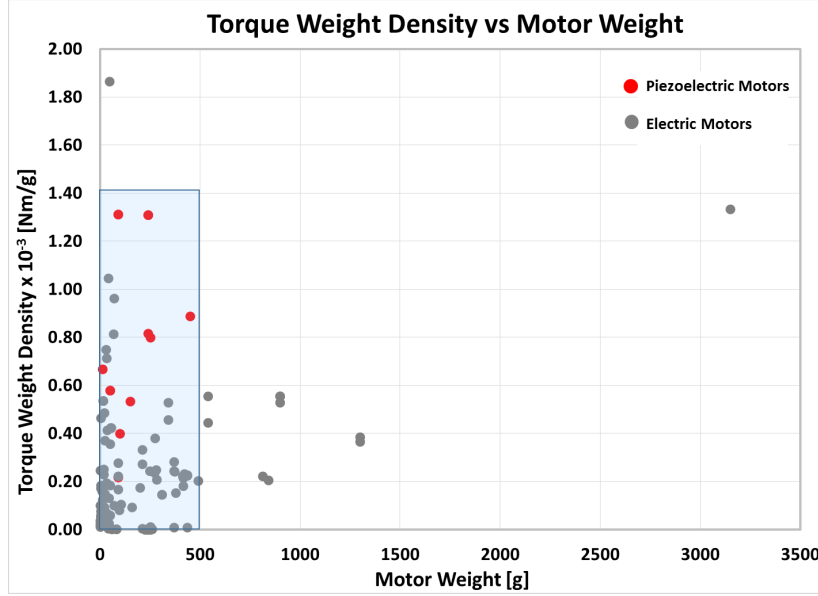


Figure 7. Weight torque density versus weight of the motor. Red dots represents piezoelectric motors. Grey dots represents electric motors. The shaded rectangular area includes motors that are going to be discussed further in Figure 8.

When considering a motor’s length scale such as motor diameter, at a small diameter range, piezoelectric motors produce larger torque density than electric motors; while, at a larger diameter range, limited numbers of piezoelectric motors are available. The larger torque density produced from scaled down piezoelectric motors compared to electric motors was shown and explained by Watson et al. [7]. The motor diameter to be discussed is limited to 50 mm for a cylindrical shape. The reason that the motor’s diameter is limited to 50 mm in this paper is that if the diameter is larger than 50 mm, the motor tends to get very heavy and use more space on the satellite wall which will limit the amount of the payload. A trend can be shown that the majority of electric motors produce small scale torque density, Figures 9 and 10. When comparing between the motors’ output torque density with respect to the motors’ density, the piezoelectric motors exhibit larger torque density with respect to their density within a similar density range, Figure 11. From Figure 4 to Figure 11, it can be concluded that the motors’ geometric characteristics and input power, i.e. weight, volume, density and linear dimension, such as a diameter, play a significant role in output torque values; and piezoelectric motors perform better than electric motors when geometric characteristics and input power are taken into consideration. The plots of torque density, shown in Figure 6 to Figure 10, show common characteristics in that the groups of motors fall into the same motor volume, motor weight and motor diameter. This is because these motors of similar volume, weight and diameter that produce various output torques are what is offered in the marketplace.

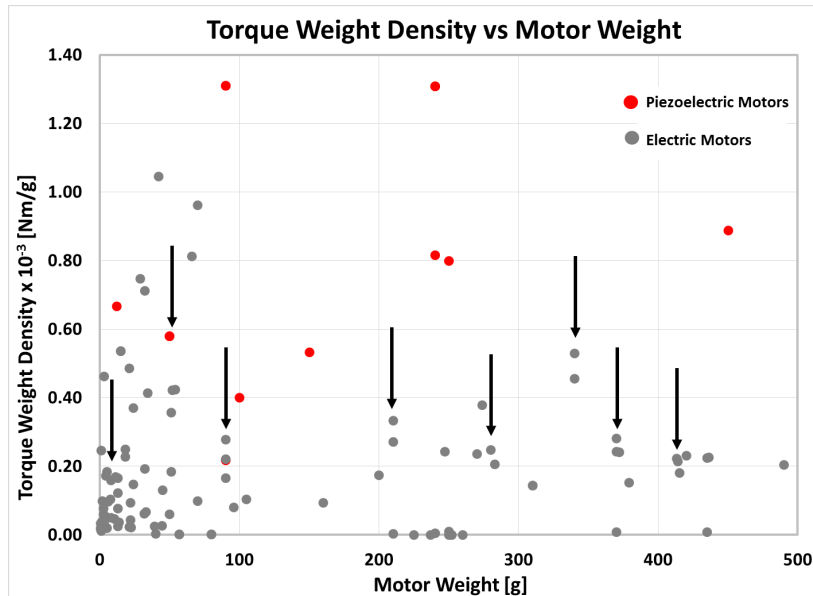


Figure 8. Weight torque density versus weight of the motor enlarged area from the shaded rectangular in Figure 7. Red dots represents piezoelectric motors. Grey dots represents electric motors. The arrows indicate groups of common motor volumes.

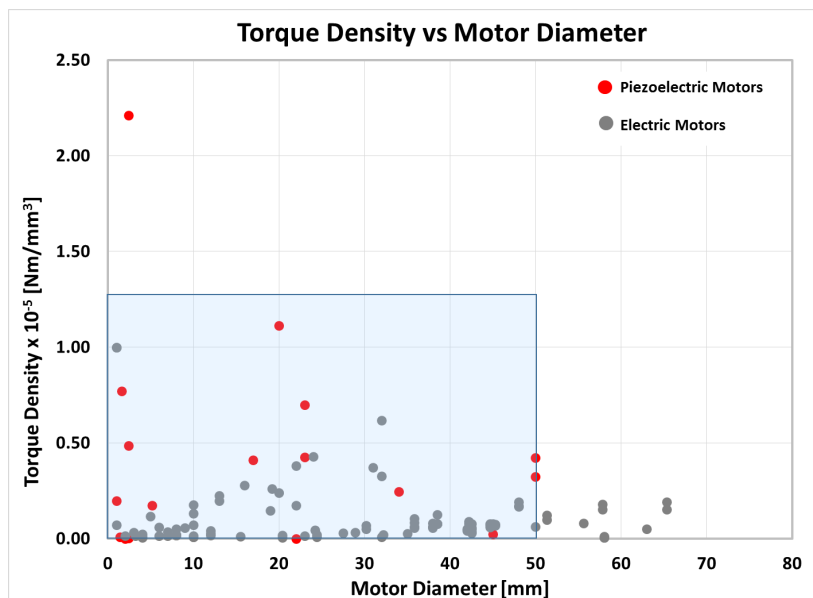


Figure 9. Torque density versus diameter of the motor. Red dots represents piezoelectric motors. Grey dots represents electric motors. The shaded rectangular area includes motors that are going to be discussed further in Figure 10.

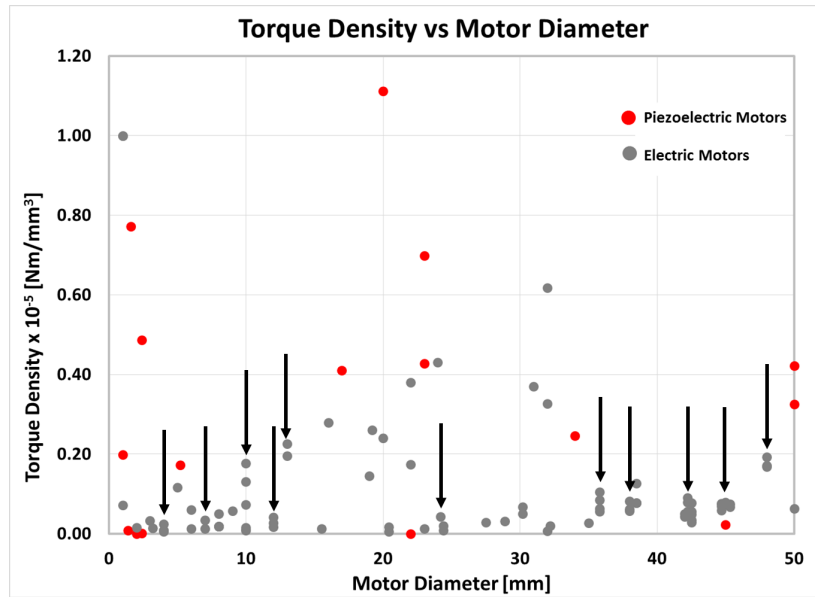


Figure 10. Torque density versus diameter of the motor enlarged area from the shaded rectangular in Figure 9. Red dots represents piezoelectric motors. Grey dots represents electric motors. The arrows show groups of common motor volumes.

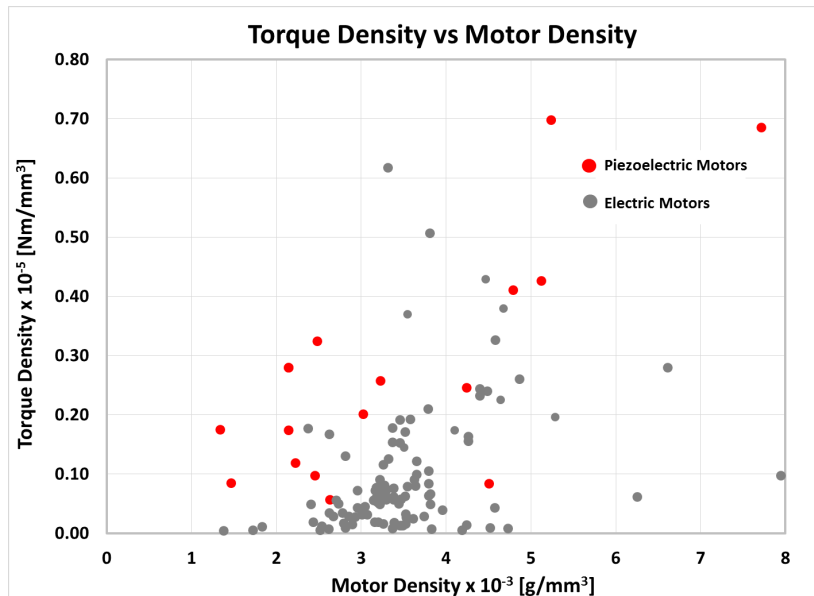


Figure 11. Torque density versus motor density. Red dots represents piezoelectric motors. Grey dots represents electric motors.

4 Heliogyro-configured Solar Sail CubeSat

A 6U CubeSat is comprised of three 2U CubeSats attached along at least one 2U face wherein the 2U CubeSat measures 100 x 200 x 100 mm. Two rolls of solar sail blades are accommodated in two 2U outer units of the 6U CubeSat, denoted as a solar sail propulsion unit. This solar sail propulsion unit is comprised of motor control electronics, rechargeable batteries and anything else associated with solar sail operation. The central 2U unit is envisioned to house the communication, on-board data handling, Electric Power System, Attitude Determination and Control System, experimental instrument package etc., Figure 12. Each solar sail reel is mounted to the satellite wall via a bearing and a motor. A motor is used to deploy and retract the solar sail blade. The motor location that will be discussed throughout this paper is mounted in the middle of the 2U CubeSat wall as shown in Figure 12. When the satellite door is opened, a solar sail is deployed out as shown in Figure 13.

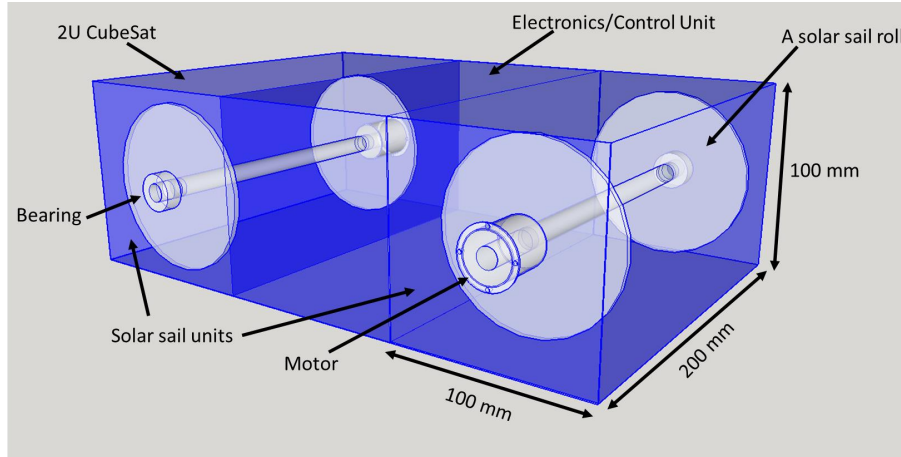


Figure 12. 6U CubeSat with two deployment mechanisms at the outer 2U boxes and one electronics/control unit is in the middle.

A thin film solar sail blade ($2 \mu\text{m}$ thick) is wrapped around a shaft, and as the shaft is rotated, the blade is deployed outward or retracted depending on the rotational direction of the shaft and reel. It is estimated that the inner shaft diameter of the solar sail roll is 10 mm and the solar sail outer roll is going to be approximately 80 mm as shown in Figure 14. The pertinent solar sail material properties are shown in Table 3. It is estimated for an ideal case that the solar sail roll is 160 mm wide along the 2U CubeSat length. The authors used the solar sail width of 160 mm here in order to maximize the total solar sail area and to seek motors in the market that can meet these extreme requirements as well as being capable of delivering a high enough torque (discussed later in the paper) to reel out the solar sail and stay within an extreme limited space provided. If the total length of the motor plus the bearing on the

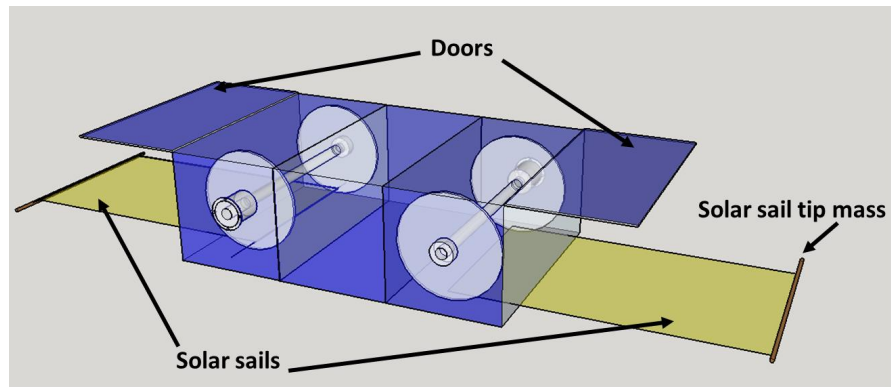


Figure 13. Extended solar sails with tip masses at the two ends.

opposite side, Figure 12, are greater than 4 cm, a right-angle gearhead may be a better option to meet the specification. Moreover, a motor set fixed at the CubeSat corner with a pulley system to rotate the solar sail shaft may be considered for the limited space provided.

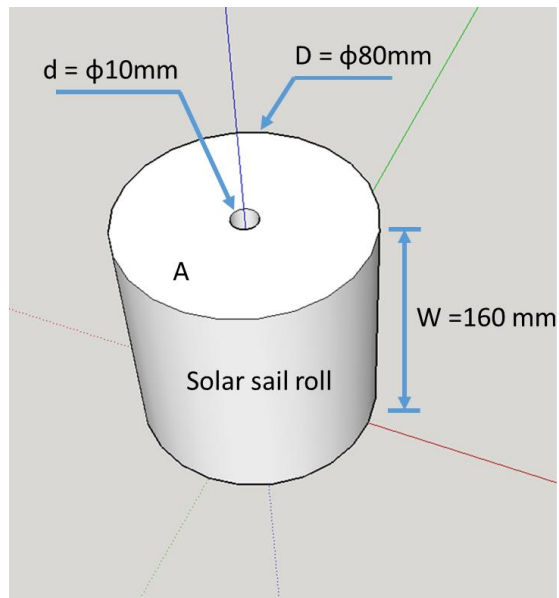


Figure 14. A solar sail roll with an outer diameter of 90 mm and an inner diameter of 10 mm. 'D' and 'd' represent outer and inner diameters, respectively. The width of the solar sail roll is 160 mm.

Solar Sail Material Properties (Kapton)	Value
Thickness (t)	2 μm
Density	1.5 [g/cm ³]

Table 3. Solar Sail Material Properties (Kapton)

The total area of the solar sail roll, area 'A' in Figure 14, determined by subtraction of the outer diameter roll from the inner diameter shaft, must be equal to the solar sail length multiplied by its thickness, Equation 1.

$$L \times t = \Pi\left(\frac{D^2}{4} - \frac{d^2}{4}\right) \quad (1)$$

where, 'L' is the solar sail length, 't' is the solar sail thickness, 'D' is the solar sail roll outer diameter and 'd' is the solar sail roll inner diameter. Thus, the length of the solar sail when fully deployed can be calculated from:

$$L = \frac{\Pi\left(\frac{D^2}{4} - \frac{d^2}{4}\right)}{t} \quad (2)$$

This total length is assumed such that the air is pumped out from the solar sail thin film roll. Therefore, it is assumed that there is no gap between adjacent solar sail thin film. The mass of the solar sail roll can be calculated by:

$$m = \rho \times V = \rho \times (\Pi \times W \times \left(\frac{D^2}{4} - \frac{d^2}{4}\right)) \quad (3)$$

where 'm' is the solar sail roll mass, ρ is the solar sail density, 'V' is the solar sail volume, 'W' is the solar sail roll width, 'D' is the outer diameter of the solar sail roll and 'd' is the inner diameter of the solar sail roll, or it is the solar sail shaft diameter. Since a motor is used to deploy the solar sail, it is required to calculate the torque requirement working against the solar sail roll. Therefore, it is assumed that the solar sail is fully deployed and the CubeSat is rotating at 2 rpm, and the drive assembly is required to furl the solar sail blade. Looking at the top view of the CubeSat with a fully extended solar sail, a centrifugal force from the tip of the solar sail towards the CubeSat is calculated as shown in Figure 15(top) with an equation

$$F_n = m \times \omega^2(L/2) \quad (4)$$

where F_n is a centrifugal force towards the CubeSat, 'm' is total mass of the solar sail roll, ω is angular speed of the CubeSat [rad/sec] and 'L' is the solar sail total extended length. A torque required to pull back the solar sail blade is calculated from Figure 15(bottom).

$$\tau = F_n \times r = F_n \times (d/2) \quad (5)$$

From Figure 14 and Table 3, the total solar sail length, when it is fully extended, is 2.47 kilometers (Equation 2). From Equation 3, the solar sail mass is 1.187 kilograms. The rotational speed of the CubeSat is 2 rpm, thus its angular speed ' ω ' is calculated to be 0.2094 [rad/sec]. From the above results, the torque required (Equation 5) from the motor is 0.32 Nm.

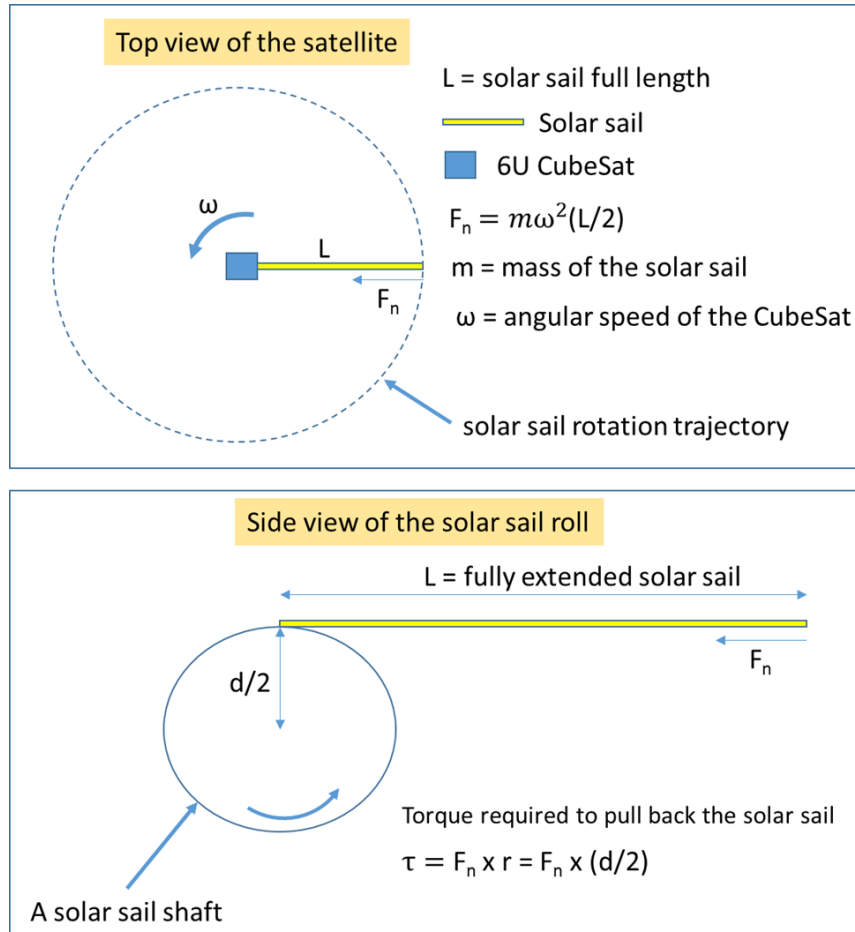


Figure 15. (Top): a top view of a CubeSat with fully extended solar sail. A dashed circle represents a rotational trajectory of the tip of the solar sail while the CubeSat rotates. (Bottom) a side-view of a solar sail roll shaft with fully extended solar sail.

4.1 Motors and Gearheads for a Solar Sail 6U CubeSat

This section describes a method to select a small scale motor to be used in a two-blade Heliogyro solar sail 6U CubeSat. The motor is required to deploy and adjust the length of the solar sails at a controlled rate. The required starting torque (at zero speed which can be considered as a stall torque) to deploy the solar sail was calculated to be 0.32 Nm,

the maximum deployment speed would be 3 rpm. A safety factor taking into account the solar sail spool weight, the motor output torque will be degraded with mission; the required torque is approximated to be 0.8 Nm. The motors to be considered in this selection are those presented in the preceding section. Since the small scale motors cannot provide such a high torque up to 0.8 Nm, a gearhead is required to increase the torque as well as to reduce the motor speed down to 3 rpm. Only an in-line gearhead connected to the motor is considered in this document, other viable options, such as right angle gearheads or pulley systems are beyond the scope of this paper's baseline analysis, as they tend to be custom made. However, not all commercial motor manufacturers provide gearheads for their motors, especially the piezoelectric motors because their speed is already low (but still higher than our requirement), and they are normally used as a direct drive. However, the commercially available piezoelectric motors still need gearheads to reduce the speed down to meet our requirements. The gearhead selected from Maxon Precision Motors meets the two most important parameters for this application, i.e. the reduction ratio and the available continuous torque. The gearhead selection process with a Maxon brushless motor, Figure 16, and a Maxon gearhead, Figure 17, is as follows.

EC 32 flat Ø32 mm, brushless, 15 Watt

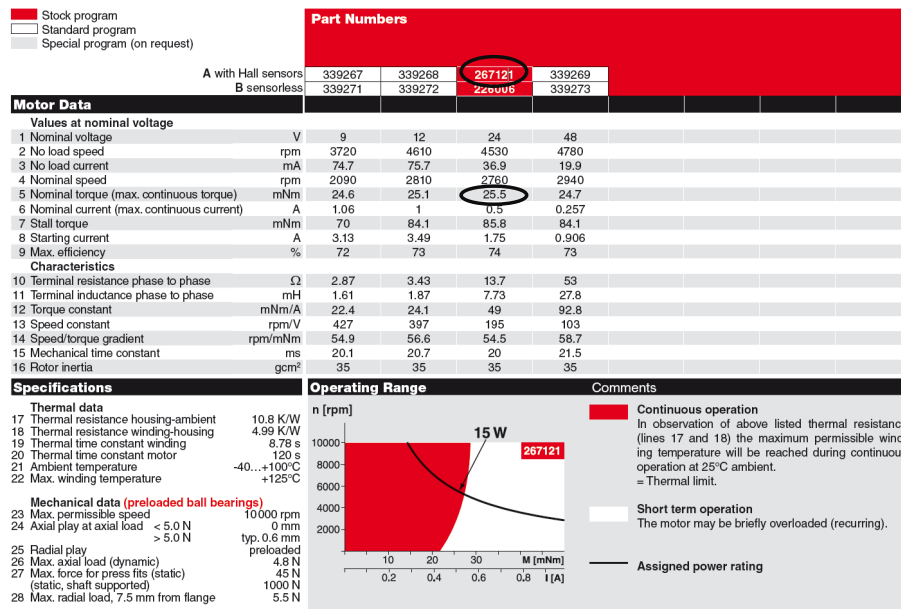


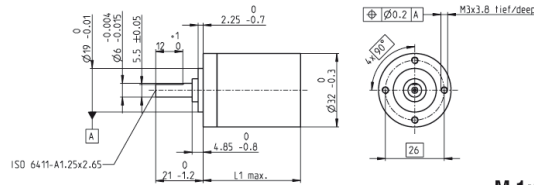
Figure 16. Brushless Maxon motor selection example. The motor part number 267121 is selected for this example (with permission from Maxon Precision Motors USA.)

A motor speed reduction is calculated from a reduction ratio,

Planetary Gearhead GP 32 C Ø32 mm, 1.0–6.0 Nm

Ceramic Version

maxon gear



Technical Data	
Planetary Gearhead	straight teeth
Output shaft	stainless steel
Shaft diameter as option	8 mm
Bearing at output	ball bearing
Radial play, 5 mm from flange	max. 0.14 mm
Axial play	max. 0.4 mm
Max. permissible axial load	120 N
Max. permissible force for press fits	120 N
Sense of rotation, drive to output	=
Recommended input speed	< 8000 rpm
Recommended temperature range	-40...+100°C
Number of stages	1 2 3 4 5
Max. radial load, 10 mm from flange	90 N 140 N 200 N 220 N 220 N

Option: Low-noise version

M 1:2

	166930	166933	166938	166939	166944	166949	166954	166959	166962	166967	166972	166977
Stock program												
Standard program												
Special program (on request)												
Part Numbers	166931	166934	166940	166945	166950	166955	166960	166963	166968	166973	166978	166983
1 Reduction	3.7:1	14:1	33:1	51:1	111:1	246:1	492:1	762:1	1181:1	1972:1	2829:1	4380:1
2 Reduction absolute	39.5	67.2	99.2	179.9	423.4	846.8	1270.2	1905.3	2857.9	4654.7	7062.1	10893.2
3 Max. motor shaft diameter	mm 6	6	6	6	6	6	6	6	6	6	6	6
Part Numbers	166932	166935	166941	166946	166951	166956	166961	166964	166969	166974	166979	166984
1 Reduction	4.8:1	18:1	66:1	123:1	295:1	591:1	886:1	1329:1	2000:1	3300:1	5000:1	7500:1
2 Reduction absolute	24.6	63.4	162.4	294.3	737.5	1475.0	2212.5	3318.8	5000.0	7500.0	11250.0	16875.0
3 Max. motor shaft diameter	mm 4	4	4	4	4	4	4	4	4	4	4	4
Part Numbers	166936	166942	166947	166952	166957	166962	166965	166970	166975	166980	166985	166990
1 Reduction	23:1	86:1	159:1	411:1	836:1	1672:1	3344:1	6688:1	13376:1	26752:1	53504:1	107008:1
2 Reduction absolute	576	1479	2853	7349	14700	29400	58800	117600	235200	470400	940800	1881600
3 Max. motor shaft diameter	mm 4	4	4	4	4	4	4	4	4	4	4	4
Part Numbers	166937	166943	166948	166953	166958	166963	166966	166971	166976	166981	166986	166991
1 Reduction	28:1	103:1	190:1	458:1	706:1	1412:1	2824:1	5648:1	11296:1	22592:1	45184:1	90368:1
2 Reduction absolute	185	658	1256	3148	4722	9444	18888	37776	75552	151104	302208	604416
3 Max. motor shaft diameter	mm 3	3	3	3	3	3	3	3	3	3	3	3
4 Number of stages	1	2	2	3	3	4	4	5	5	5	5	5
5 Max. continuous torque	Nm 1	3	3	6	6	6	6	6	6	6	6	6
6 Intermittently permissible torque at gear output	Nm 1.25	3.75	3.75	7.5	7.5	7.5	7.5	7.5	7.5	7.5	7.5	7.5
7 Max. efficiency	% 80	75	75	70	70	60	60	60	60	50	50	50
8 Weight	g 118	162	162	194	194	226	226	226	258	258	258	258
9 Average backlash no load	0.7	0.8	0.8	1.0	1.0	1.0	1.0	1.0	1.0	1.0	1.0	1.0
10 Mass inertia	gcm ² 1.5	0.8	0.8	0.7	0.7	0.7	0.7	0.7	0.7	0.7	0.7	0.7
11 Gearhead length L1	mm 26.5	36.4	36.4	43.1	43.1	49.8	49.8	49.8	56.5	56.5	56.5	56.5

Figure 17. Maxon gearhead part number 166960 is selected for this example. (with permission from Maxon Precision Motors USA.)

$$i_{Gear} = \frac{n_{Motor}}{n_{Load}} \quad (6)$$

where i_{Gear} is the reduction ratio of the gearhead, n_{Motor} is the nominal motor speed, and n_{Load} is the speed that the gearhead will produce to the load. The nominal speed is a suggested continuous speed of this motor with load. A larger speed such as a no load speed, or the maximum speed at which this motor can run may also be used for the calculation.

Once the desired reduction ratio is determined, it can be used to select a gearhead. As a rule, the next smaller available gearhead reduction ratio of the selected gear type will be used if an exact reduction ratio is not available. This is to keep the gearhead as small as possible, i.e. fewer number of gear stages, to meet the requirements.

Next is to calculate output torque at the load by taking into account gearhead efficiency and reduction ratio,

$$M_{Load} = M_{Motor} \times \eta_{Gear} \times i_{Gear} \quad (7)$$

where i_{Gear} is a reduction ratio of the gearhead (determined in Equation 6), M_{Motor} is a nominal motor torque, M_{Load} is a torque that the gearhead will provide to the load when connected to this motor, and η_{Gear} is the gearhead efficiency.

After these calculations, both the M_{Load} value and the maximum continuous torque of the gearhead value must be larger than the required torque to deploy/furl the solar sail blade. As an example, a Maxon motor part number 267121 is selected for this application because of the highest maximum continuous torque and it provides the highest efficiency when compared to other EC32 flat motors as shown in Figure 16. The motor part number 267121 possesses a load speed requirement of 3 rpm and the motor nominal speed is 2760 rpm, Figure 16. The speed reduction ratio was calculated to be 920:1.

With a reduction ratio of 920:1, a reduction ratio of 913:1 is selected and shown as part number 166960, Figure 17. The output torque at the gearhead to the load is

$$M_{Load} = 25.5mNm \times 0.6 \times 913 = 13.968mNm = 13.97Nm \quad (8)$$

4.2 Results of Motors and Gearheads Selection for a Solar Sail 6U CubeSat

The term 'a motor set' will be used throughout this document to represent a motor when attached to a gearhead. This section shows and discusses results of various motor sets, described in the preceding section, associated with selected gearheads according to the selection procedures described in the previous subsection. Commercially available miniature gearheads are limited in the market. In particular, there are no miniature gearheads produced for all piezoelectric and electric motors. Due to this limitation, the authors selected these gearheads from Maxon Precision Motors because Maxon Precision Motors provides a variety of gearheads to accommodate dimensions and reduction ratios for their products. The authors selected these gearheads as close to the motors' diameters and required speed reduction ratios as possible due to the limited numbers of products available in the market. Thus, to be precise with the gearhead selection of all non-Maxon Precision Motors, customized gearheads are necessary for each motor. Selection criteria for choosing a motor set are:

- 1) the output torque at the load (produced from a gearhead when attached with a motor) must be larger than 0.8 Nm
- 2) the maximum continuous torque of the gearhead must be larger than 0.8 Nm
- 3) the motor set weight should be within 150 grams
- 4) the total motor set length should be within 40 mm. This motor may not be directly connected to the solar sail shaft but it might be connected to a right angle motion transmission system, and
- 5) brushed motors are not of interested for this application

The brushed motors do not fit with this application because of fine powder that would be generated during operation contaminating the satellite. The output torque produced from a gearhead, when attached to a motor, indicates the maximum output torque that the motor set can deliver when considering that the gearhead is running at its maximum efficiency. The motor set weight limitation was approximately 5-6% of the weight limitation of a 2U CubeSat. Weight limitation of a 2U CubeSat is 2.66 kg, since a 1U CubeSat's weight limitation is 1.33 kg (3 lbs. per U) [38]. Since 5% of 2.66 kg is 133 grams, most of the small scale motors plus gearheads that can provide such a high torque of 0.8 Nm are expected to be quite heavy, indicating that they may not meet this criteria. The authors decided to take approximately 5.5% of the 2U CubeSat weight limitation, which is 146 grams. Thus, a motor set weight limitation of 150 grams is going to be used for this application. The weight combination of a solar sail roll plus a motor set is 1.84 kg which is approximately 70% of the allowable weight, leaving 30% for a solar sail spool and other subsystems inside this solar sail unit such as

a release mechanism to open the satellite door and the satellite structure etc. By looking at the overall drive system torque-volume density, it can be observed that piezoelectric motor sets exhibit smaller volume than most of the electric motor sets but their torque volume density was considerably smaller than brushed motors, Figure 18.

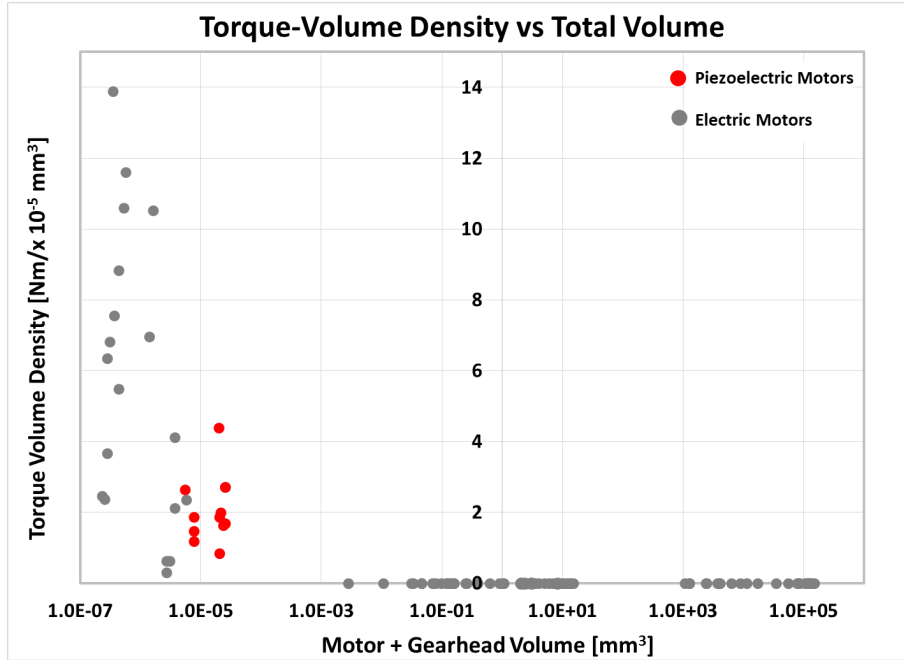


Figure 18. Motor + gearhead volume versus torque volume density of motor sets. The electric motors with motor + gearhead volume less than $1 \times 10^{-3} \text{ mm}^3$ are brushed motors. The rest of the electric motors with total volume larger than $1 \times 10^{-3} \text{ mm}^3$ are brushless and stepper motors.

It can be observed that most of the electric motors show a very large percentage volume increase when a gearhead is needed to reduce the speed and to increase the torque up to meet the operational requirements, Figure 19. The term percentage of the total weight (or volume) increase indicates how much of the total weight (or volume) is increased when a gearhead is attached to the motor compared to an individual motor itself. There are some electric motors that show a similar trend of percentage of total weight and volume increase when compared to sets of piezoelectric motors, but those electric motor sets are brushed motors and will not be considered further. It can be observed that piezoelectric motor sets show lower percentage increase of total weight and volume than the rest of electric motor sets. From this observation, piezoelectric motors do not require as much space and weight from the gearheads to reduce speed and increase the torque as electric motors require. However, all of the piezoelectric motor sets, USSR-series motors, that exhibit the lower trend of total weight and volume increase, shown in Figure 19, do not meet length requirement and they are too heavy. The two piezoelectric motor

sets, PiezoLEG 30mNm and 50mNm, meet weight requirement and their length is quite short. However, their output torque at the load are 0.146 and 0.234 Nm, with maximum continuous output torques of 0.1 and 0.75 Nm, respectively. Hence, PiezoLEG 30mNm and 50mNm do not meet output torque requirements.

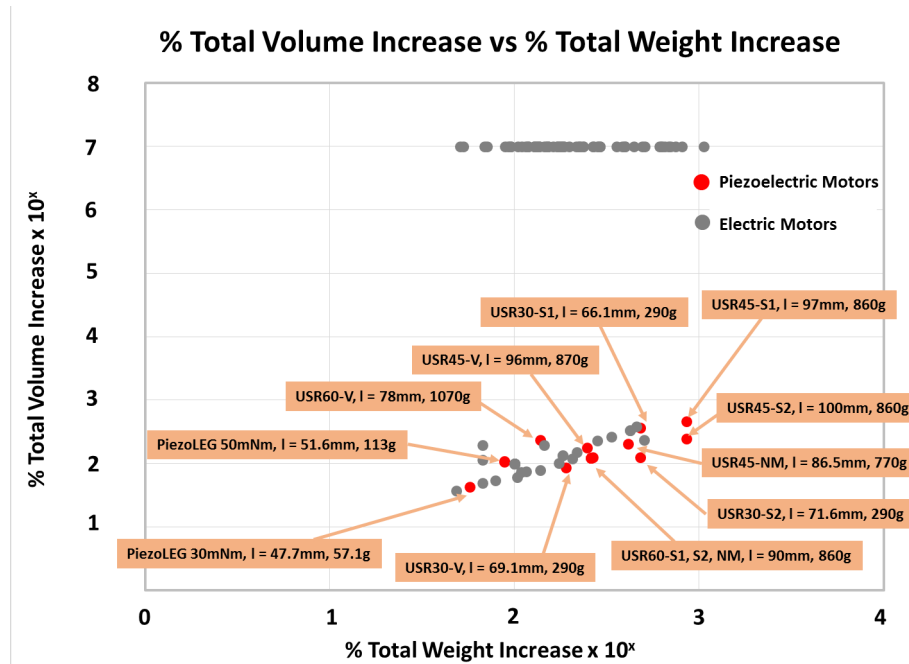


Figure 19. Percentage of total weight increase of motor sets and percentage of total volume increase of motor sets. Group of electric motors locate nearby piezoelectric motors are brushes motors. The number with a unit 'mm' indicates the total length of the motor set.

Large ranges of output torque, from motor sets, and maximum continuous torque from gearheads are shown in Figure 20. A smaller range of these output torques are going to be considered for ease of analysis and these are shown in Figure 21. Two torque profiles, one horizontal line and one vertical line, show minimum torque requirements for this application, i.e. 0.8 Nm. Any motor sets located inside these profiles, i.e. torques below 0.8 Nm, will not qualify for this application. The motor names, their total length, and weight are identified at each motor set except brushes motors that have no motor set information. It can be observed that most of piezoelectric motors and their gearheads do a better job in producing larger output torques than electric motors plus their gearheads. By looking at each qualified output torque, the total length of some piezoelectric motor sets, such as USR60-S1-V-NM are too long to be accommodated inside this 2U satellite that allow maximum solar sail blade width. It can be observed that the length of all of electric motor sets exceed our requirements, i.e. 40 mm. There are a number of motor sets that are heavier than 150 grams such as USR60-S1-V-NM,

USR30-S1-V, EC flat Maxon, EGEHS-12 and EGEH-12-H Johnson Electric. The two electric motor sets that possess similar lengths and weights are within 150 grams are EC32 flat Maxon and E4HS-12 Johnson Electric motors. However, the EC20 flat Maxon motor is considered to be the best compromise when output torques are considered. Comparing the length and weight to the E4HS-12 Johnson Electric motors, it is the shortest drive system, with a total length of 62.4 mm, and weighs the least, i.e. 109 grams.

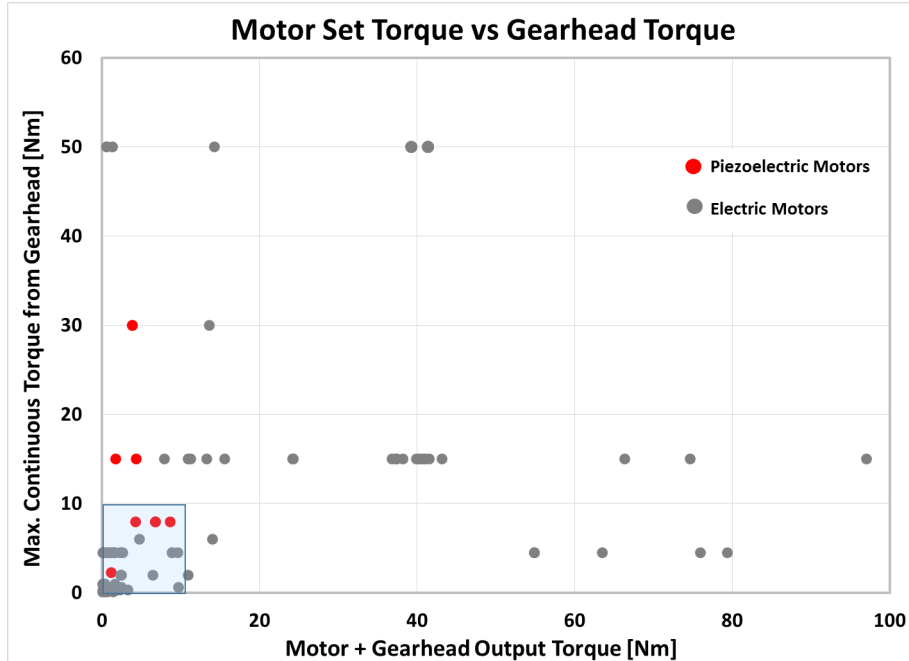


Figure 20. Motors plus gearheads output torque and maximum continuous torque produced from gearheads. The shaded rectangle includes motors that are going to be further discussed in Figure 21.

A large range of motor set output torque values compared to the motor set total weight are shown in Figure 22. A smaller range of output torque values compared to the total weight are shown in Figure 23. A torque profile of 0.8 Nm, shown as a vertical line, indicates the minimum torque requirement. A weight profile, shown as a dotted horizontal line, indicates the boundary of acceptable weight, i.e. 150 grams. Any motor sets that fall below the weight profile line and produces an output torque larger than 0.8 Nm will be considered. From these requirements, it can be observed that there are three motor sets that show a large output torque and weigh below 150 grams, but, they are still longer than the 40 mm length requirement. These motor sets are EC-13 flat, EC-max 16 and EC-20 flat Maxon motors. By comparing all three motor sets, the EC-13 Maxon shows a light weight of 49 grams, while its length is approximately similar to the other two motor sets. However, this EC-13 Maxon motor does not meet the maximum continuous output torque

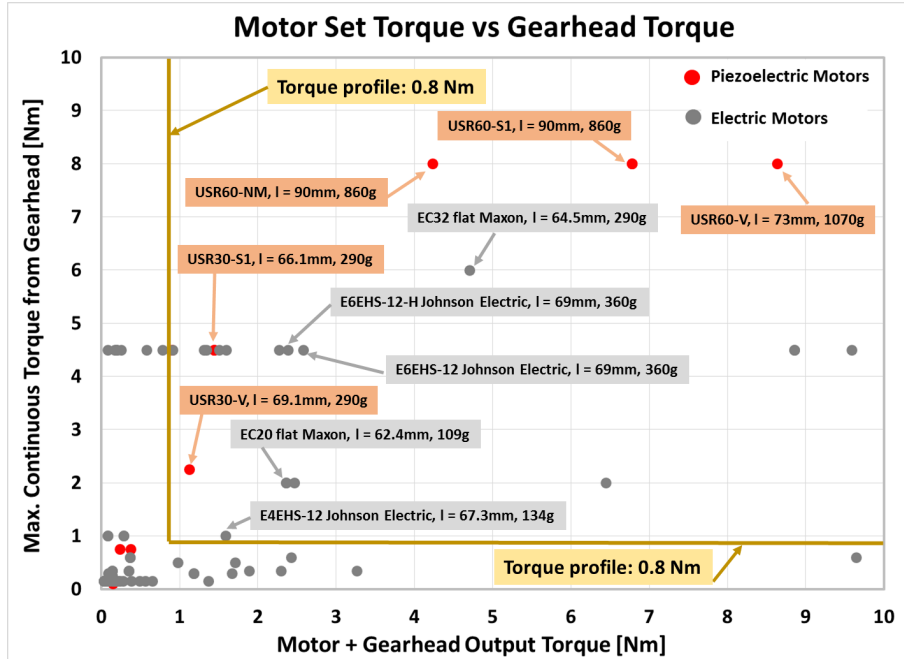


Figure 21. Small range of output torque of motor sets and maximum continuous torque from gearheads. Two torque profile lines are used to separate motor sets that generate lower output torque than requirement of 0.8 Nm. The number with a unit 'mm' indicates the total length of the motor set.

from the gearhead, Figure 21, so this motor cannot be used in this application. Similarly, EC-max 16 motor set does not meet the maximum continuous torque from its gearhead. The gearhead of the EC-max 16 flat motor exhibits 0.6 Nm maximum continuous output torque. The gearhead of EC-20 flat motor set exhibits 2 Nm which meets the requirement.

Gearhead maximum continuous torques and motor set output torques, when compared to total motor set lengths, are shown in Figures 24 and 25. It can be observed that no motor set falls into the acceptable region of producing larger output torque than required with a total length within 40 mm.

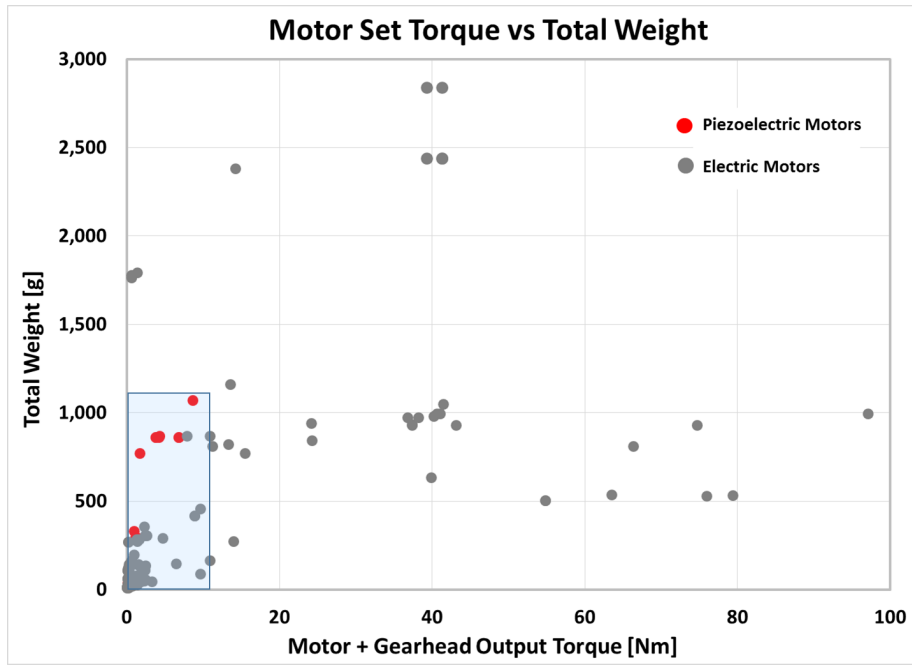


Figure 22. Comparison between output torques of motors plus gearheads versus their total weight. The shaded rectangle includes motors that are going to be further discussed in Figure 23.

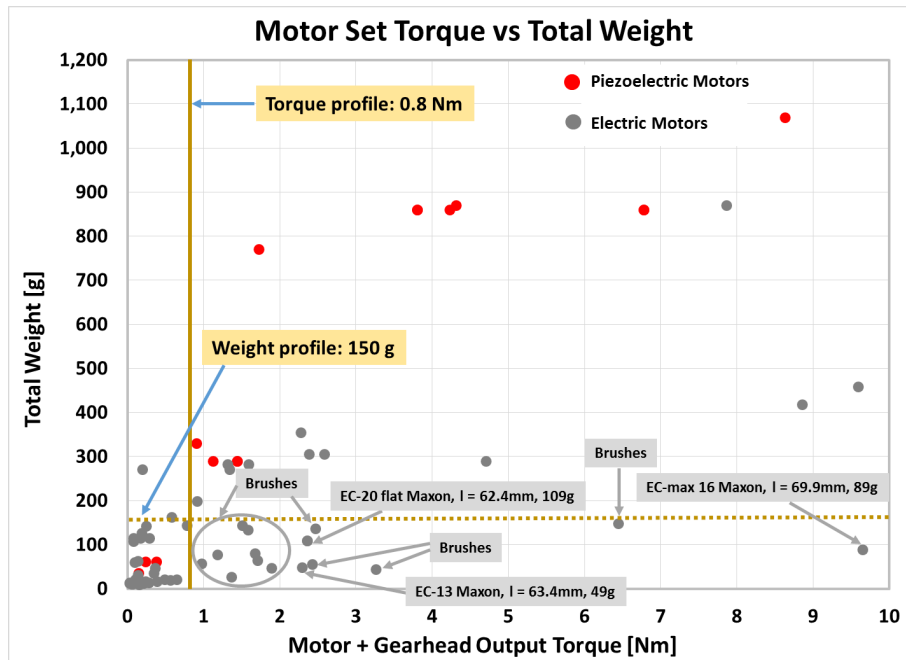


Figure 23. Small range of output torque derived from motor sets compared to the total weight. A torque profile line is used to separate motor sets that generate lower output torque than requirement of 0.8 Nm. A motor set weight profile line is used as a boundary of maximum allowable motor sets weight of 150 gram.

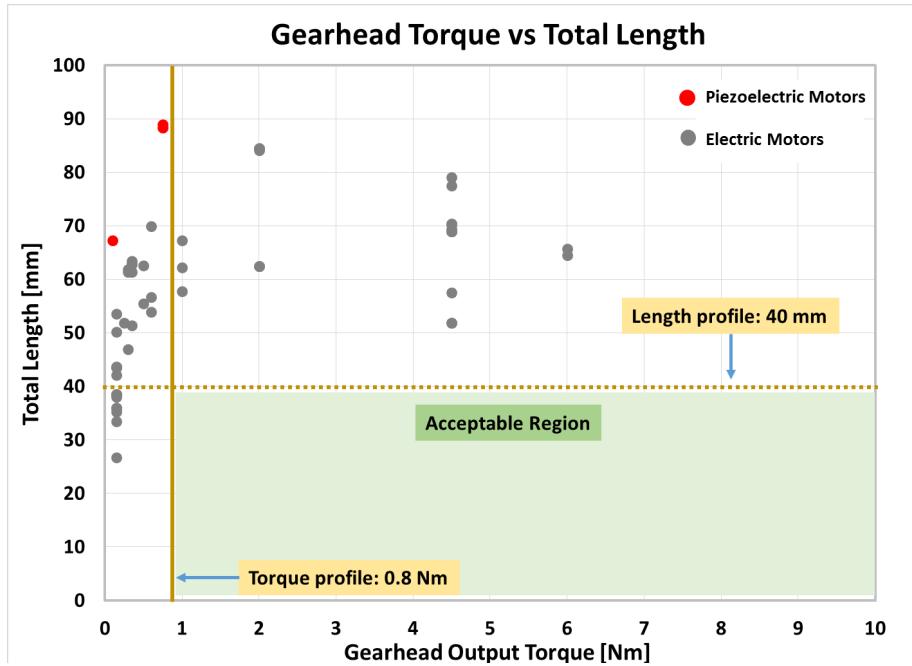


Figure 24. Gearhead output torque compared to total length of a motor plus a gearhead. A torque profile line is used to separate motor sets that generate lower output torque than requirement of 0.8 Nm. A motor set length profile line is used as a boundary of maximum allowable motor set length.

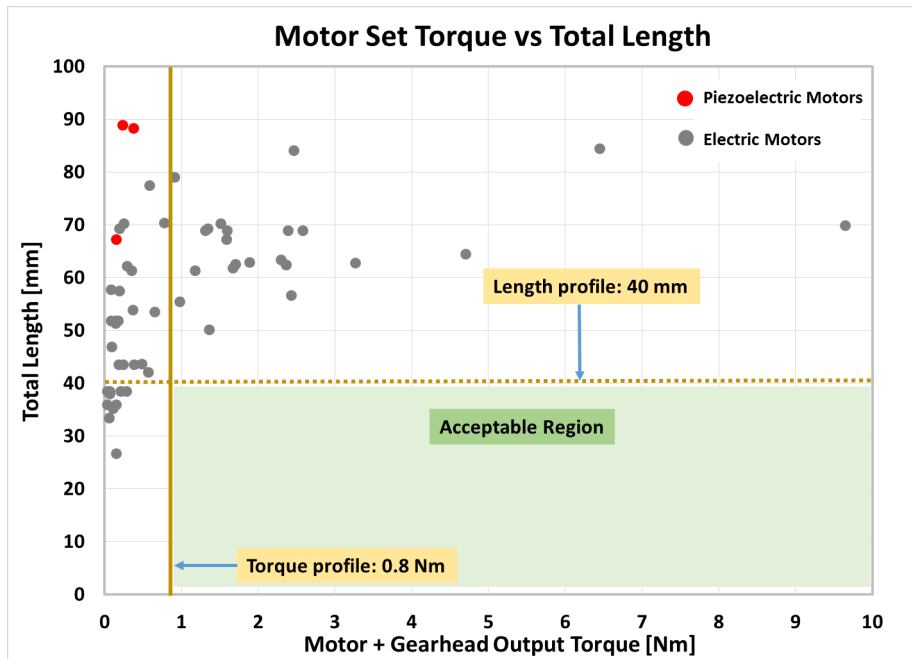


Figure 25. Motor sets output torque compared to total their lengths. A torque profile line is used to separate motor sets that generate lower output torque than requirement of 0.8 Nm. A motor set length profile line is used as a boundary of maximum allowable motor set length.

5 Results

Commercial electric DC and piezoelectric ultrasonic motors were compared along with research-type piezoelectric ultrasonic motors. The output torque of piezoelectric ultrasonic motors was determined to be greater than electric motors. Moreover, piezoelectric ultrasonic motors required less input power than electric motors to produce larger output torque. Piezoelectric ultrasonic motors required less space and weighed less than electric motors. However, the piezoelectric motors were not chosen for this application because none of miniaturized piezoelectric motors available in the market met our size and weight limitations. In addition, the developed research-type piezoelectric motors are still immature for space-rated applications.

Since none of the small scale motors available in the market exhibit the high required torque at low speed, a gearhead was determined to be necessary to produce the required output parameters. A motor plus a gearhead, the drive system, must be used to deploy a roll of solar sail. Gearhead selection procedures are discussed in subsection 4.1. From analysis in subsection 4.2, none of the commercial small scale motors available in the market met all of the requirements. However, there were some motors that met the requirements of the output torque using a gearhead that exceeded the minimum torque requirement, and the maximum continuous output torque. There were some motors that were lighter than the maximum weight limitation. However, none of the motor sets met the length requirement. The best compromise (low weight and capable of deliver required output torque) set of motor plus a gearhead was the EC20 flat Maxon motor series that can deliver the required output torque with a weight of 109 grams. The length was still too long, i.e. 62.4 mm. The gearhead of EC-20 flat motor set exhibited 2 Nm which meets the requirement and requires input power of 3W which was in an acceptable range for a 6U CubeSat power. The output torque at the load was determined to be 2.36 Nm.

An illustration of the EC20 flat Maxon motor plus a gearhead mounted to the solar sail roll spindle is shown in Figure 26. On the opposite side of the spindle is a bearing to allow rotation while the motor and the gearhead rotate. The whole mechanism is confined in a length of 200 mm. It can be seen that after taking into account the motor and the gearhead length and leaving some space for two spindle discs and a bearing, an available width for the solar sail roll is approximately 100 mm wide. The solar sail width of 100 mm is very narrow when a large sail area is required to compensate for the satellite weight in order to achieve large characteristic acceleration of the solar sail satellite. The theoretical characteristic acceleration is a metric to determine the solar sail performance at 1 AU (astronomical unit) and is highly dependent on the ratio of the

solar sail area to the payload mass [39]. However, this EC20 flat Maxon motor was chosen because of the availability of the gearhead. By assuming the outer diameter of the solar sail is 80 mm, the inner diameter of the solar sail roll is 10 mm, Figure 14, and the solar sail roll width of 100.6 mm, Figure 26, the characteristic acceleration of this 6U Solar Sail CubeSat is 0.509 mm/s^2 . This characteristic acceleration is considered to be large when compared to the IKAROS [40] solar sail spacecraft and a NanoSail-D [41] solar sail 3U CubeSat with characteristic acceleration of 0.0053 mm/s^2 and 0.02 mm/s^2 , respectively.

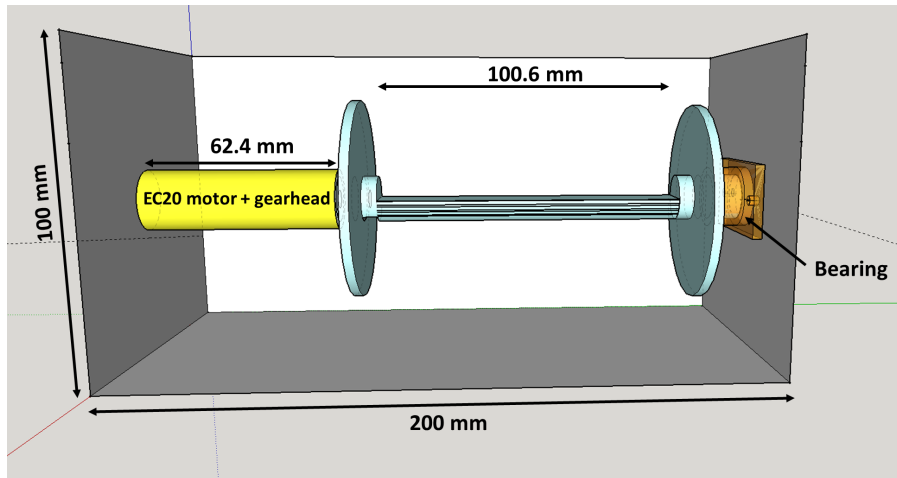


Figure 26. EC20 Maxon motor plus a gearhead is mounted to the solar sail roll spindle and the opposite side is a bearing. The EC20 Maxon motor plus a gearhead was chosen for this application because it can deliver required torque and its weight is lower than requirement. The spindle diameter is 80 mm.

To shorten the total length of the motor set, a right-angle gearhead may be considered, for example with piezoelectric or electric motors. However, these right-angle gearheads available in the market by the time this report was written (March 2015) have very low reduction ratios [42–47]. Low reduction ratios mean the speed will be reduced by a low factor. To reduce the motor speed range of thousands to more than 10^5 revolution per minute (rpm) [1–3] down to 3 rpm for this unique application, an in-line gearhead, usually with higher reduction ratios, is still needed. For those off-the-shelf right angle gearheads available in the market at the time this report was written, it may not significantly reduce the total length of the motor set with the required additional in-line gearhead. A recommendation is to customize a right angle gearhead for each selected motor, especially piezoelectric motors because they already possess low speed, as a lower number of gear stages are required, when compared to electric motors. Using a piezoelectric motor set with customized gearhead would be another good option because its total length can be very short, and its weight can be small.

One of the motor selection criteria is to limit the motor diameter to 50 mm. The reason is that if the diameter is larger than 50 mm, the motor tends to get very heavy and use more space on the satellite wall which will limit the amount of the payload. For example, if a Maxon motor EC 60 flat ϕ 60 mm brushless (diameter of 60 mm) is used, the motor's weight (not including a gearhead to reduce its speed) is 470 grams. If a Maxon motor EC 90 flat ϕ 90 mm brushless (diameter of 90 mm) is used, the motor's weight (not including a gearhead to reduce its speed) is 600 grams. The diameter of 60 mm is very large when it is mounted on the satellite wall with a dimension of 100 x 100 mm. Similarly, the diameter of 90 mm is too large for a 100 x 100 mm satellite wall as there will be no space for the flange to mount the motor.

The solar sail roll considered in this paper has outer and inner diameters of 80 and 10 mm, respectively, and a width of 100 mm. These dimensions make this solar sail weigh 742 grams (28% of the total allowable 2U CubeSat weight of 2.66 kg). Taking only a roll of solar sail weight into account, there are 1920 grams left for other mechanisms and motor's battery/controlling system and other scientific payloads. The motors' weight (without a gearhead) of 600 and 900 grams already takes 23% and 34% of the total allowable weight of a 2U CubeSat (2.66 kg), respectively. While the selected motor EC20 flat Maxon plus a gearhead weigh only 109 grams, it takes only 4% of the total 2U CubeSat allowable weight. Thus, the motor diameter for a limited space as shown in this application should be limited to within 50 mm.

6 Conclusions

This report compares the performance of commercial electric DC and piezoelectric ultrasonic motors as well as research-type piezoelectric ultrasonic motors. The most critical parameters for the ongoing space application to deploy and control a solar sail 6U CubeSat are output torque and input power. Motor selection methods to deploy and control a solar sail 6U CubeSat were also discussed by comparing the performance of small scale electric and piezoelectric ultrasonic motors. A small scale range was limited to within $3 \times 10^2 \text{ cm}^3$ ($3 \times 10^5 \text{ mm}^3$), the diameter was limited to 50 mm for a cylindrical shape and the motors' weight was required to be less than 500 grams. The driving parameters were motor's stall torque, between 0.8 Nm, and a weight not exceeding 150 grams. None of the motors discussed here were capable of working as a direct drive system because of the speed requirement being too low, 3 rpm, and the required load torque being as high as 0.8 Nm for such small scale motor. Thus, a gearhead must be attached to each motor to reduce the speed and increase the torque. A gearhead selection method was discussed in this paper and motor sets plus selected gearheads were

compared. A motor plus a gearhead must meet the following five requirements 1) the output torque at the load must be at least 0.8 Nm, 2) maximum continuous torque from the gearhead must be 0.8 Nm or greater, 3) the motor set weight should be no greater than 150 grams, 4) the total motor set length should be within 40 mm, and 5) brushed motor configurations should not be considered due to limited lifetime, low efficiency, and contamination issues. It was concluded that none of the motors (piezoelectric motors and electric motors) plus gearheads met all the five requirements. There was only one small scale electric motor that showed the most optimized outcome (low weight and capable of deliver required output torque) but still had a total length (a motor length plus a gearhead length) that exceeded the requirement. If a right angle gearhead system that was built specifically for miniature piezoelectric motors was used, then the piezoelectric motors would be a good motor set candidate when compared to electric motors due to the lower speed and higher torque produced from piezoelectric motors alone. The gearhead used for piezoelectric motors could have lower gear stages than that required by electric motors, resulting in a shorter and lighter gearhead. Thus, a customized gearhead system should be designed, rather than a motor, as the best approach to cost effectively enable the full capabilities of a 2U solar sail propulsion system in terms of deployed blade area and reel control.

Appendix Lists of 130 Commercial Motors Shown in this Paper

Commercial Piezoelectric Motors

Piezo LEG Rotary 30mNm, 50mNm, 80mNm and Piezo LEG Wave [48]

USR60-S1, USR60-S2, USR60-NM, USR60-V, USR30-S1, USR30-S2, USR30-NM, USR30-V, USR45-S1, USR45-S2, USR45-NM, USR45-V [10]

Commercial DC Motors Maxon Precision Motors [1]

RE-13 Brushes, RE-max 13 Brushes, A-Max 19 DC Brushes, A-Max 22 DC Brushes, RE-max 21 Brushes, RE-max 24 Brushes, DCX- 22s Brushes, EC 13 Brushless, EC-max 16 Brushless, EC 10 flat Brushless, EC 9.2 flat Brushless, EC 20flat Brushless, EC 20 flat brushless, EC 32 flat brushless, EC 32 flat brushless and EC 45 flat brushless

Commercial DC Motors Precision Microdrive [8]

Model: 103-100, 104-000, 104-001, 104-003, 106-002, 107-001, 108-103, 108-104, 108-106
Model: 110-001, 110-002, 110-003, 112-001, 112-002, 116-101
Model: 120-002, 120-100, 124-001, 124-002
Model: 132-100, 132-201, 136-201, 136-402

Commercial DC Motors Johnson Electric [9]

DF315XLLG-021, DC651(2)XLLG-022, DC651(2)XLLG-023, DC651-P-001, DC751(2)LSG-022, DC751(2)XLLG-011, DC751(2)XLLG-021, DC751(2)XLLG-022, DC751(2)XLLG-023, DC751(2)XLLG-024, DC751(2)XLLG-025, DC771(2)XLLG-012, DC771(2)XLLG-022, DC771(2)XLLG-023, DC771(2)XLLG-025, DC781(2)XLLG-021, DC971-P-001, E4EHS-12, E5EHS-12, E5EHS-12-H, E6EHS-12, E6EHS-12-H , E7IHM-24, E8IHM-14, E8IHM-18, E8IHM-22, E9IWS-28, E7IHL-120, E7IHL-240, E10DE-240-001, E10DE-240-002, E10IE-240-001

Commercial DC Motors Crouzet [3]

Part number 82710001, 82720001, 82860011, 82740001, 82810017, 82810501, 82830009, 80140510, 80180505, 80180506, 80140511, 80140512, 80120301, 82910001, 82900, 829200, 829300 2 phases, 829300 4 phases, 829400 2 phases, 829400 4 phases, 82910501, 82910502

Commercial DC Motors AUTOM [2]

AFF-K10WD, AFF-K20WD, AFF-030PA, AFF-050SK, AFF-130SH,
AFF-180SH, AFF-K30WD, AFF-M10PA, AFF-M20PA, AFF-M30PA,
AFF-N20VA, AFF-N30VA, ARF-130CH, ARF-300CA, ARF-300CH,
ARF-330TA, ARF-370CA, ARF-370CB, ARF-500TB, ARF-1220CA, ARF-
1230CA

References

1. Maxon Precision Motors. URL <http://www.maxonmotorusa.com>, accessed May, 18, 2015.
2. Autom Tech. Industry C., LTD. URL <http://www.autom.cn/>, accessed May, 18, 2015.
3. Crouzet Motors. URL <http://www.crouzet.com>, accessed May, 18, 2015.
4. Hughes, A.; and Drury, B.: Electric Motors and Drives: Fundamentals, Types and Applications, 4th Edition. 2013.
5. Wiwattananon, P.; and Bryant, R. G.: Literature Review on Miniature Piezoelectric Motors. *NASA Technical Memorandum*, vol. NASA/TM-2015-XXXX, 2015.
6. Liu, D. K.-C.; Friend, J.; and Leo, L.: A brief review of actuation at the micro-scale using electrostatics, electromagnetics and piezoelectric ultrasonics. *Acoustical Science and Technology*, vol. 31, no. 2, 2010, pp. 115–123. URL <http://dx.doi.org/10.1250/ast.31.115>.
7. Watson, B.; Friend, J.; and Yeo, L.: Piezoelectric ultrasonic micro/milli-scale actuators. *Sensors and Actuators A: Physical*, vol. 152, no. 2, 2009, pp. 219 – 233. URL <http://dx.doi.org/10.1016/j.sna.2009.04.001>.
8. Precision Micro Drives. URL <http://www.precisionmicrodrives.com/>, accessed April, 21, 2014.
9. Johnson Electric. URL www.johnsonelectric.com, accessed April, 21, 2014.
10. Fukoku Shinsei Motors. URL <http://www.mmech.com/ultrasonic-motors/fukoku-shinsei-motors>, accessed April, 21, 2014.
11. Piezo Motor. URL www.piezomotor.se, accessed April, 21, 2014.
12. Parker Motion. URL http://www.parkermotion.com/literature/pdf/pg235_eng_tech.pdf, accessed April, 21, 2014.
13. Williams, A. L.; and Brown, W. J.: Piezoelectric motor. Apr. 13 1948. US Patent 2,439,499.
14. Dong, S.; Cagatay, S.; Uchino, K.; and Viehland, D.: A 'Center-Wobbling' Ultrasonic Rotary Motor Using a Metal Tube-Piezoelectric Plate Composite Stator. *Journal of Intelligent Material Systems and Structures*, vol. 13, no. 11, 2002, pp. 749–755. URL <http://dx.doi.org/10.1177/1045389X02013011006>.

15. Koc, B., U.-K.; and Tressler, J. F.: A Miniature Piezoelectric Rotary Motor Using two Orthogonal Bending Modes of a Hollow Cylinder. *International Conference on New Actuators*, 2000, pp. 242–245.
16. Morita, T.; Kuribayashi Kurosawa, M.; and Higuchi, T.: A cylindrical micro ultrasonic motor using PZT thin film deposited by single process hydrothermal method ($\phi=2.4$ mm, $L=10$ mm stator transducer). *IEEE Transactions on Ultrasonics, Ferroelectrics and Frequency Control*, vol. 45, no. 5, 1998, pp. 1178–1187. URL <http://dx.doi.org/10.1109/58.726441>.
17. Morita, T.; Kurosawa, M. K.; and Higuchi, T.: Cylindrical micro ultrasonic motor utilizing bulk lead zirconate titanate (PZT). *Journal of Japanese Applied Physics*, vol. 38, no. 5B, 1999, pp. 3347–3350. URL <http://dx.doi.org/10.1143/JJAP.38.3347>.
18. Morita, T.; Kurosawa, M. K.; and Higuchi, T.: A cylindrical shaped micro ultrasonic motor utilizing PZT thin film (1.4 mm in diameter and 5.0 mm long stator transducer). *Sensors and Actuators A: Physical*, vol. 83, no. 1, 2000, pp. 225–230. URL [http://dx.doi.org/10.1016/S0924-4247\(99\)00388-X](http://dx.doi.org/10.1016/S0924-4247(99)00388-X).
19. Kanda, T.; Makino, A.; Suzumori, K.; Morita, T.; and Kurosawa, M.: A cylindrical micro ultrasonic motor using a micro-machined bulk piezoelectric transducer. *IEEE Ultrasonics Symposium*, vol. 2, 2004, pp. 1298–1301. URL <http://dx.doi.org/10.1109/ULTSYM.2004.1418028>.
20. Kanda, T.; Makino, A.; Ono, T.; Suzumori, K.; Morita, T.; and Kurosawa, M. K.: A micro ultrasonic motor using a micro-machined cylindrical bulk PZT transducer. *Sensors and Actuators A: physical*, vol. 127, no. 1, 2006, pp. 131–138. URL <http://dx.doi.org/10.1016/j.sna.2005.10.056>.
21. Koc, B.; Cagatay, S.; and Uchino, K.: A piezoelectric motor using two orthogonal bending modes of a hollow cylinder. *IEEE Transactions on Ultrasonics, Ferroelectrics and Frequency Control*, vol. 49, no. 4, 2002, pp. 495–500. URL <http://dx.doi.org/10.1109/58.996568>.
22. Cagatay, S.; Koc, B.; Moses, P.; and Uchino, K.: A Piezoelectric Micromotor with a Stator of $\phi=1.6$ mm and $l=4$ mm Using Bulk PZT. *Journal of Japanese Applied Physics*, vol. 43, no. 4R, 2004, pp. 1429–1433. URL <http://dx.doi.org/10.1143/JJAP.43.1429>.
23. Park, S.; and He, S.: Standing wave brass-PZT square tubular ultrasonic motor. *Ultrasonics*, vol. 52, no. 7, 2012, pp. 880–889. URL <http://dx.doi.org/10.1016/j.ultras.2012.02.010>.

24. Shinsei. URL <http://www.shinsei-motor.com/English/>, accessed April, 21, 2014.
25. Kurosawa, M.; Takahashi, M.; and Higuchi, T.: Ultrasonic linear motor using surface acoustic waves. *IEEE Transactions on Ultrasonics, Ferroelectrics and Frequency Control*, vol. 43, no. 5, 1996, pp. 901–906. URL <http://dx.doi.org/10.1109/58.535493>.
26. Kurosawa, M. K.; Chiba, M.; and Higuchi, T.: Evaluation of a surface acoustic wave motor with a multi-contact-point slider. *Smart Materials and Structures*, vol. 7, no. 3, 1998, pp. 305–311. URL <http://dx.doi.org/10.1088/0964-1726/7/3/005>.
27. Takasaki, M.; Osakabe, N.; Kurosawa, M. K.; and Higuchi, T.: Miniaturization of surface acoustic wave linear motor. *Ultrasonics Symposium*, Institute of Electrical and Electronics Engineers Inc., vol. 1, 1998, pp. 679–682.
28. Kurosawa, M. K.: State-of-the-art surface acoustic wave linear motor and its future applications. *Ultrasonics*, vol. 38, no. 1, 2000, pp. 15–19. URL [http://dx.doi.org/10.1016/S0041-624X\(99\)00087-6](http://dx.doi.org/10.1016/S0041-624X(99)00087-6).
29. Takasaki, M.; Kuribayashi Kurosawa, M.; and Higuchi, T.: Optimum contact conditions for miniaturized surface acoustic wave linear motor. *Ultrasonics*, vol. 38, no. 1, 2000, pp. 51–53. URL [http://dx.doi.org/10.1016/S0041-624X\(99\)00093-1](http://dx.doi.org/10.1016/S0041-624X(99)00093-1).
30. Shigematsu, T.; Kurosawa, M. K.; and Asai, K.: Nanometer stepping drives of surface acoustic wave motor. *IEEE Transactions on Ultrasonics, Ferroelectrics and Frequency Control*, vol. 50, no. 4, 2003, pp. 376–385. URL <http://dx.doi.org/10.1109/TUFFC.2003.1197960>.
31. Zhang, H.; Dong, S.-x.; Zhang, S.-y.; Wang, T.-h.; Zhang, Z.-n.; and Fan, L.: Ultrasonic micro-motor using miniature piezoelectric tube with diameter of 1.0 mm. *Ultrasonics*, vol. 44, 2006, pp. e603–e606. URL <http://dx.doi.org/10.1016/j.ultras.2006.05.064>.
32. Yoon, C.-B.; Lee, S.-M.; Kim, H.-E.; and Lee, K.-W.: Windmill-type ultrasonic micromotor fabricated by thermoplastic green machining process. *Sensors and Actuators A: Physical*, vol. 134, no. 2, 2007, pp. 519–524. URL <http://dx.doi.org/10.1016/j.sna.2006.05.040>.
33. Takeda, D.; Yamaguchi, D.; Kanda, T.; Suzumori, K.; and Noguchi, Y.: An Ultrasonic Motor Using a Titanium Transducer for a Cryogenic Environment. *Journal of Japanese Applied Physics*, vol. 52, no. 7S, 2013, pp. 07HE13–1–07HE13–6. URL <http://dx.doi.org/10.7567/JJAP.52.07HE13>.

34. Kurosawa, M.; and Ueha, S.: Hybrid transducer type ultrasonic motor. *IEEE Transactions on Ultrasonics, Ferroelectrics and Frequency Control*, vol. 38, no. 2, 1991, pp. 89–92. URL <http://dx.doi.org/10.1109/58.68464>.
35. Nakamura, K.; Kurosawa, M.; and Ueha, S.: Characteristics of a hybrid transducer-type ultrasonic motor. *IEEE Transactions on Ultrasonics, Ferroelectrics and Frequency Control*, vol. 38, no. 3, 1991, pp. 188–193. URL <http://dx.doi.org/10.1109/58.79602>.
36. Wajchman, D.; Liu, K.-C.; Friend, J.; and Yeo, L.: An ultrasonic piezoelectric motor utilizing axial-torsional coupling in a pretwisted non-circular cross-sectioned prismatic beam. *IEEE Transactions on Ultrasonics, Ferroelectrics and Frequency Control*, vol. 55, no. 4, 2008, pp. 832–840. URL <http://dx.doi.org/10.1109/TUFFC.2008.717>.
37. Drexler, K. E.: Productive nanosystems: the physics of molecular fabrication. *Physics education*, vol. 40, no. 4, 2005, pp. 339–346. URL <http://dx.doi.org/10.1088/0031-9120/40/4/003>.
38. NASA CubeSat Initiative. URL http://www.nasa.gov/directorates/heo/home/CubeSats_initiative.html, accessed March, 21, 2015.
39. McInnes, C. R.: *Solar Sailing*. Springer-Praxis, Chichester, UK, 1999.
40. IKAROS. URL <http://www.jspec.jaxa.jp/e/activity/ikaros.html>, accessed November, 3, 2014.
41. Johnson, L.; Whorton, M.; Heaton, A.; Pinson, R.; Laue, G.; and Adams, C.: NanoSail-D: A solar sail demonstration mission. *Acta Astronautica*, vol. 68, no. 56, 2011, pp. 571 – 575. URL <http://www.sciencedirect.com/science/article/pii/S0094576510000597>, special Issue: Aosta 2009 Symposium.
42. Maxon Right Angle. URL http://www.maxonmotorusa.com/maxon/view/news/PRESSRELEASE-Right_angle_spiroid_gear_launch, accessed May, 18, 2015.
43. Right Angle Gearhead, Stock Drive Products. URL http://www.sdp-si.com/estore/coverpg/right_angle_drives.htm, accessed May, 18, 2015.
44. Miniature Right Angle Drives, Torque Transmission. URL <http://www.torquetrans.com/miniature-right-angle-drives>, accessed May, 18, 2015.

45. Right Angle Gear Drives, Designatronics. URL <http://www.designatronics.com/products-and-solutions/right-angle-drives.php>, accessed May, 18, 2015.
46. Crown Gear Right Angle Gearbox, Zero Max. URL <http://www.zero-max.com/crown-gear-right-angle-gearbox-c-22-1-en.html>, accessed May, 18, 2015.
47. Miniature Sprial Bevel Gearboxes Right Angle Power Transmission, GamWeb. URL http://www.gamweb.com/downloads/MiniBevelGearboxes_L_Series.pdf, accessed May, 18, 2015.
48. MicroMo. URL <http://www.micromo.com/>, accessed May, 9, 2014.

REPORT DOCUMENTATION PAGE				Form Approved OMB No. 0704-0188	
<p>The public reporting burden for this collection of information is estimated to average 1 hour per response, including the time for reviewing instructions, searching existing data sources, gathering and maintaining the data needed, and completing and reviewing the collection of information. Send comments regarding this burden estimate or any other aspect of this collection of information, including suggestions for reducing this burden, to Department of Defense, Washington Headquarters Services, Directorate for Information Operations and Reports (0704-0188), 1215 Jefferson Davis Highway, Suite 1204, Arlington, VA 22202-4302. Respondents should be aware that notwithstanding any other provision of law, no person shall be subject to any penalty for failing to comply with a collection of information if it does not display a currently valid OMB control number.</p> <p>PLEASE DO NOT RETURN YOUR FORM TO THE ABOVE ADDRESS.</p>					
1. REPORT DATE (DD-MM-YYYY) 01-08 - 2015		2. REPORT TYPE Technical Memorandum		3. DATES COVERED (From - To)	
4. TITLE AND SUBTITLE Performance Comparisons and Down Selection of Small Motors for Two-Blade Heliogyro Solar Sail 6U CubeSat			5a. CONTRACT NUMBER		
			5b. GRANT NUMBER		
			5c. PROGRAM ELEMENT NUMBER		
6. AUTHOR(S) Wiwattananon, Peerawan; Bryant, Robert G.			5d. PROJECT NUMBER		
			5e. TASK NUMBER		
			5f. WORK UNIT NUMBER 432938.08.01.07.01		
7. PERFORMING ORGANIZATION NAME(S) AND ADDRESS(ES) NASA Langley Research Center Hampton, VA 23681-2199			8. PERFORMING ORGANIZATION REPORT NUMBER L-20567		
9. SPONSORING/MONITORING AGENCY NAME(S) AND ADDRESS(ES) National Aeronautics and Space Administration Washington, DC 20546-0001			10. SPONSOR/MONITOR'S ACRONYM(S) NASA		
			11. SPONSOR/MONITOR'S REPORT NUMBER(S) NASA-TM-2015-218784		
12. DISTRIBUTION/AVAILABILITY STATEMENT Unclassified - Unlimited Subject Category 31 Availability: NASA STI Program (757) 864-9658					
13. SUPPLEMENTARY NOTES					
14. ABSTRACT This report compiles a review of 130 commercial small scale motors (piezoelectric and electric motors) and almost 20 researched-type small scale piezoelectric motors for potential use in a 2 blades Heliogyro Solar Sail 6U CubeSat. In this application, a motor and gearhead (drive system) will deploy a roll of solar sail thin film (2 um thick) accommodated in a 2U CubeSat (100 x 200 x 100 mm) housing. The application requirements are: space rated, output torque at full deployment of 0.8 Nm, reel speed of 3 rpm, drive system weight limited to 150 grams, diameter limited to 50 mm, and the length not to exceed 40 mm. The 50 mm diameter limit was imposed as motors with larger diameters would likely weigh too much and use more space on the satellite wall. This would limit the amount of the payload. The motors performance are compared between small scale, volume within 3x10 ² cm ³ (3x10 ⁵ mm ³), commercial electric DC motors, commercial piezoelectric motors, and researched-type (non-commercial) piezoelectric motors extracted from scientific and product literature. The comparisons suggest that piezoelectric motors without a gearhead exhibit larger output torque with respect to their volume and weight and require less input power to produce high torque. A commercially available electric motor plus a gearhead was chosen through a proposed selection process to meet the applications design requirements.					
15. SUBJECT TERMS CubeSat; Miniature motors; Solar sail					
16. SECURITY CLASSIFICATION OF:			17. LIMITATION OF ABSTRACT	18. NUMBER OF PAGES	19a. NAME OF RESPONSIBLE PERSON
a. REPORT	b. ABSTRACT	c. THIS PAGE			STI Help Desk (email: help@sti.nasa.gov)
U	U	U	UU	44	19b. TELEPHONE NUMBER (Include area code) (757) 864-9658